FIMV IS INVOLVED IN THE FUNCTION AND REGULATION OF THE TYPE IV PILUS SYSTEM IN *PSEUDOMONAS AERUGINOSA*

FIMV IS INVOLVED IN THE FUNCTION AND REGULATION OF THE TYPE IV PILUS SYSTEM IN *PSEUDOMONAS AERUGINOSA*

By

Anthony E. Shimkoff B.Sc. (Hons)

A Thesis

Submitted to the School of Graduate Studies

in Partial Fulfillment of the Requirements

for the Degree

Master of Science

McMaster University

MASTER OF SCIENCE (2009) McMaster University

(Biochemistry and Biomedical Sciences) Hamilton, ON

TITLE: FimV is Involved in the Function and Regulation of the Type IV PIlus System in *Pseudomonas aeruginosa*

AUTHOR: Anthony E. Shimkoff

SUPERVISOR: Dr. Lori L. Burrows

NUMBER OF PAGES: 114

ABSTRACT

Immunocompromised, burned, and cystic fibrosis patients are highly susceptible to severe and chronic *Pseudomonas* infections. Extracellular virulence factors, such as type IV pili (T4P), contribute to the establishment and maintenance of infection in these hosts. T4P are hair-like appendages involved in attachment to and colonization of biotic and abiotic surfaces, DNA uptake, biofilm formation, virulence and twitching motility. In *Pseudomonas aeruginosa*, the pilus fibre—primarily composed of PilA—is directed by the inner membrane subcomplex PilM/N/O/P to PilQ, the secretin pore. FimV is an inner membrane protein that contains a periplasmic region that binds peptidoglycan and a cytoplasmic region containing tetratricopeptide repeat (TPR) protein-protein interaction domains. FimV is essential for twitching motility in *P. aeruginosa*, but its exact function is not well understood. Here we investigate the role of the cytoplasmic region of FimV in the T4P system. Co-purification studies revealed that PilM and PilG, a protein proposed to be involved in T4P chemotaxis, interact with the cytoplasmic region of FimV. Fluoresence microscopy was used to test the role of FimV in the localization of a functional PilG-YFP fusion. In the wild type, PilG is polarly localized, while in a *fimV* mutant, PilG becomes diffuse. The interactions between FimV with PilG and PilM may play a pivotal role in twitching motility as *fimV*

mutants lacking the cytoplasmic region are incapable of twitching. In this study, we have shown that FimV is interacting with components of the T4P chemotaxis system, which may be important for cAMP regulation.

ACKNOWLEDGEMENTS

Firstly I would like to thank my supervisor, Dr. Lori Burrows, for giving me the opportunity to be a graduate student in her fantastic laboratory. She taught me to use critical thinking and curiosity to help guide my research. Her words of wisdom and guidance have shaped me into a scientist. I thank her for all of the time spent in her office, talking about my project and theorizing different hypotheses, no matter how crazy they may have seemed at the time. I especially thank her for teaching me the importance of planning and designing an experiment. Her words of "measure twice, cut once" will live with me for the rest of my life.

I would also like to thank my two committee members, Dr. Marie Elliot and Dr. Murray Junop. Both of you were invaluable contributors not only to my research, but to my professional development as a scientist. You have enriched my graduate studies experience by being challenging, supportive and enlightening members of my committee and I thank you. Dr. Elliot, I thank you for the insight you provided throughout my thesis project work. The impact it had on my research may not be measurable, but my project most certainly benifited from it. Dr. Junop, the encouragement and motivation you have given me since my undergraduate schooling is something I will never forget. I hope to make you, Marie, and Lori proud in my future endeavors .

There are a few members of the Burrows Lab I would like to thank. Dr. Hania Wehbi, for training me and teaching me some of the skills that helped make me a scientist. Dr. Edie Scheurwater, for feeding my curiosity by participating in leisurely scientific discussions. Dr. Adil Khan, Dr. Melissa Ayers and Dr. Carmen Giltner for being exemplary role models for me as both a student and a researcher. Thanks to Martin Daniel-Ivad for his hard work and dedication to learning and contributing to my masters thesis and Uyen Nguyen for her wisdom and friendship. Last but not least I would like to thank Iwona Wenderska, Ylan Nguyen, and Hosam Khalil, not only for helping me in my research, but the friendships that we have built over the time we worked together. Without you three, working in the lab quite simply would not have been as enjoyable without all of you. My time in the Burrows will always be remembered as a time of hard work, but also a lot of fun. Thank you all.

ATTRIBUTIONS

Hosam Khalil and Martin Daniel-Ivad produced the fluorescent microscopy images. Hosam Khalil constructed the pET151:*pilG* and the pMarkiC:*pilG-yfp* constructs. Martin Daniel-Ivad expressed and purified FimV634 and conducted the partial proteolysis experiment in **Figure 13**. Eder Portillo constructed the pFimV-6xHis complementation construct.

TABLE OF CONTENTS

LIST OF TABLES

LIST OF FIGURES

1.0 INTRODUCTION AND BACKGROUND

1.1 *Pseudomonas aeruginosa*

Pseudomonas aeruginosa is a gram-negative, rod-shaped, motile, aerobic bacterium that grows in soil, wet lands and coastal marine habitats, as well as plant and animal tissues (Bodey et al., 1983; Nickel et al., 1985; Hardalo et al., 1997). *P. aeruginosa* is an opportunistic pathogen capable of attaching to biotic and abiotic surfaces where it can form highly resistant biofilm communities which aid in evading antimicrobial agents and host immune responses (Costerton et al., 1999). Immunocompromised, burn, and cystic fibrosis patients are most susceptible to severe and chronic *Pseudomonas* infection (Sato et al., 1988; Semmler et al., 2000). Extracellular virulence factors including lipases, phospholipases, proteases, exopolysaccharides, alkaline phosphatases, pyochelins, and type IV pili work together to establish and maintain infection in these hosts (Bodey et al., 1983). By studying these virulence factors, we may develop or discover novel drug targets and/or treatment approaches.

1.2 Type IV Pili

There are several virulence factors that contribute to the pathogenesis of *P. aeruginosa*. The production of lipases, proteases and Type IV Pili (T4P) is crucial to initiating and sustaining *Pseudomonas*

infections (Bodey et al., 1983). T4P are retractable, hair-like appendages that span the cellular envelope of the bacteria and extend out into the extracellular environment. T4P are involved in bacteriophage adsorption, DNA uptake and biofilm formation (Russell et al., 1994; Morand et al., 2004; Carbonnelle et al., 2006), however they also give the bacteria the ability to attach and colonize a wide variety of environmental surfaces, an important function for pathogenesis. T4P are commonly found in gram-negative bacteria such as *Neisseria gonorrhoeae,* enteropathogenic *Escherichia coli* and *P. aeruginosa (*Alm et al., 1996). In *Pseudomonas*, T4P are flexible, filamentous surface appendages that are 5-8 nm in diameter, several micrometers in length and are assembled at the poles of the cell (Touhami et al., 2006; Nguyen et al., 2009). The pilus fiber is a polymer composed primarily of the structural protein subunit PilA, which is held together through strong hydrophobic interactions in N-terminal region of PilA. So far, over 50 genes that are required for the regulation, assembly and function of T4P have been identified (Mattick, 2002). In addition to their role in surface attachment, T4P give bacteria the ability to move in a flagellum-independent manner termed twitching motility (Alm et al., 1996).

1.3 Twitching Motility

Twitching motility was first observed in *Acinetobacter calcoaceticus* (Lautrop, 1963) and was so named to describe the jerky movement displayed by the cells in liquid media. This form of motility is mediated by the extension, attachment, and retraction of the T4P; a three-step process powered by at least two ATPases. A study in *N. gonorrhoeae* measured the retraction force of a single pilus motor to exceed 100pN (Merz et al., 2000 and Maier et al., 2002) and more recently multiple pili were found to exert forces in the nN range (Biais et al., 2008) making T4P one of the strongest molecular machines identified to date. Twitching motility is important for virulence, as strains lacking functional T4P are hindered in their ability to infect (Costerton et al., 1999). The production of T4P is not sufficient for infection, as pilus retraction is also required for virulence (Han et al., 2008; Zolfaghar et al., 2003). In *P. aeruginosa,* PilB and PilT are ATPases responsible for the assembly and disassembly, respectively, of the pilus fiber. The two enzymes belong to the AAA+ super-family of multimeric mechanoezyme ATPases that facilitate the stable protein-protein interactions of multiprotein complexes through the hydrolysis of ATP (Morand et al., 2004; Chiang et al., 2005). Mutational analysis of the ATPases showed that *pilB* is involved in the pilin polymerization and *pilT* is involved in the retraction of the pilus by pilin depolymerization. Neither mutant has the ability to twitch, however *pilB* mutants have no observable

surface pili, whereas *pilT* mutants have greater than wild type levels of surface pili (Burrows, 2005).

1.4 Type IV Pilus Assembly Complex

P. aeruginosa has been a model organism for studying T4P and twitching motility due to the availability of genome sequences, host-vector systems for cloning and expression, and the ease by which different twitching phenotypes can be identified (Mattick, 2002). Twitching motility in *P. aeruginosa* is facilitated by an envelope-spanning complex of proteins (**Figure 1**) which includes the PilB and PilT ATPases. The PilT paralogue PilU is also thought to be involved in retraction of the pilus, as *pilU* mutants have surface pili but only limited motility (Burrows, 2005), however, the function of this ATPase is not well understood. Using fluorescent microscopy, PilB and PilT were observed to localize to both poles of the cell (Chiang et al., 2005) whereas PilU localizes to the leading pole during movement. The pilus itself is primarily composed of the major pilin subunit PilA (Strom and Lory, 1993; Nguyen et al., 2009), although more recent studies using immunogold labelling have demonstrated the incorporation of minor pilin subunits into the pilus as well (Giltner et al., 2010). The major and minor pilin subunits share sequence and structural homology. Prior to pilus formation, prepilin subunits are localized to the

inner membrane where they are processed to their mature, assembly competent form by PilD, an inner membrane prepilin peptidase.

In order for the pilus fibre to extend into the extracellular environment, it must pass through the outer membrane and peptidoglycan layer. PilQ is a 77 kDa protein encoded by *pilQ*, part of the polycistronic operon *pilMNOPQ*, and forms a homo-dodecomeric secretin pore in the outer membrane (Peabody et al., 2003; Bitter et al., 1998). Secretin complexes are ring-like structures (Koster et al., 1997; Linderoth et al., 1997; Hahn et al.,1997) that facilitate the passage of the pilus through the outer membrane. The PilQ complex is SDS- and heat resistant and can only be dissociated into PilQ monomers using phenol treatment. The secretin has a diameter of roughly 180 Å and a pore opening of 50 Å, large enough to accommodate the pilus fiber (Bitter et al., 1998; Nguyen et al., 2009). The pilotin protein PilF, an outer-membrane lipoprotein, assists in the assembly of PilQ multimers, as *pilF* mutants are incapable of PilQ multimerization (Koo et al., 2008). In *P. aeruginosa*, PilQ monomers localize to the inner membrane whereas PilQ multimers localize to the outer membrane (Koo et al., 2008).

While PilQ functions in the outer membrane; PilMNOP form an inner membrane sub-complex (Ayers et al., 2009; Sampaleanu et al., 2009; Tammam et al., in revision). Bioinformatics analysis suggests that PilM is a cytoplasmic protein with an actin-like fold, PilN and PilO are type

II membrane proteins and PilP is an inner membrane lipoprotein. Complementation of various *pilM/N/O/P* mutant strains revealed that the proteins depend upon one another for stability (Ayers et al., 2009). The periplasmic domains of PilN and PilO can be co-purified as a stable heterodimer , providing additional support for the concept of an inner membrane assembly sub-complex (Sampaleanu et al., 2009). The current model for T4P extension involves the PilMNOP inner membrane sub-complex working in concert with PilC, a putative inner membrane 'platform' protein (Carbonnelle et al., 2006), to coordinate ATPase activity and direct the pilus fibre to the secretin pore formed by PilQ multimers. However, the way in which the pilus and other components of the multiprotein T4P complex traverse the peptidoglycan layer is not well understood.

1.5 Regulation of the T4P System by the *pil-chp* gene cluster and Vfr

Motile bacteria use chemotaxis systems to sense changes in the concentration of chemicals in their environment to elicit a behavioral response. The "*pil-chp*" cluster encodes a chemotaxis system (**Figure 1**) that regulates pilus-mediated twitching motility. The genes in this cluster are *pilG/H/I/J/KchpA/B/C* (Whitchurch et al. 2004; Darzins et al., 1993,1994,1995). The products of these genes are predicted to form a complex chemosensory system resembling the one that controls flagellum rotation in bacteria such as *E. coli* (Kato et al. 2008). Based on the

flagellar model, the putative membrane-bound methyl-accepting chemotaxis (MCP) protein PilJ senses an extracellular stimulus, initiating a cascade of events that leads to the phosphorylation of the response regulator PilG; this final event is believed to activate the T4P machinery.

Recently, the Pil-Chp proteins have been associated with another layer of T4P regulation in *P. aeruginosa.* Vfr (Virulence Factor Regulator) is a transcriptional regulator related to the catabolite repressor protein (CRP) and regulates genes involved in Type 2 and 3 Secretion, flagellar and T4P systems in response to changes in levels of intracellular cAMP (Fulcher et al., 2010; Kanack et al., 2004). A transposon mutant screen for regulators of the major adenylate cyclase CyaB, which synthesizes cAMP, revealed that *fimV* and genes in the *pil-chp* cluster positively control cAMP levels and thus affect Vfr-regulated virulence gene expression. Among the targets of Vfr is the *pilMNOPQ* operon, helping to explain the previously reported observation that PilMNOPQ levels are decreased in a *fimV* mutant (Wehbi et al., 2011). A study on the affects of FimV in the Type 2 Secretion system reported that *vfr* expression was reduced in a *fimV* mutant (Michel et al., 2011), which would have global affects on many virulence factors of *P. aeruginosa.*

1.6 FimV

In *P. aeruginosa,* the *fimV* gene locus is located between *usg-1* and *truA* genes which are involved in the biosynthetic pathway leading to cell wall precursors, and in tRNA modification, respectively (Semmler et al., 2000; Ahn et al., 2004). In *E. coli*, *usg-1* is located directly upstream of *truA* forming an operon, evidence that *fimV* was acquired through horizontal gene transfer in *P. aeruginosa* (Semmler et al., 2000; Ahn et al., 2004). FimV is a 96.9 kDa protein, with an N-terminal peptidoglycan-binding LysM domain, a coiled coil region, a proline/alanine rich domain, a transmembrane domain and a highly acidic C-terminus; the last ~50 residues are highly conserved among FimV orthologues (**Figure 2**). A *P. aeruginosa* transposon mutant screen for mutants with abnormal twitching motility phenotypes led to the identification of *fimV* (Semmler et al., 2000). From this transposon mutant screen, two phenotypes emerged; a group of mutants lacking twitching motility, represented by the S4 mutant, and one mutant, S125, with smaller and irregular twitching zones. In the S4 group, the transposon insertion occurred either close to the start codon or in the middle of the gene, resulting in a severely truncated and/or unstable FimV product compared to wild type. In the S125 mutant, the transposon insertion occurred 230 base pairs upstream of the stop codon, presumably resulting in a truncated but partially functional protein. Both of these *fimV* mutant groups were deficient in pilus fibre assembly. Using various

concentrations of IPTG to induce *fimV* expression from a complementation construct, Semmler et al. (2000) found that 0.01-0.03 mM concentrations of IPTG were required for normal twitching motility, but higher concentrations resulted in loss of twitching and elongation of the cell that was predicted to be the cause for the reduction in motility. This genetic study demonstrated the involvement of FimV in the T4P assembly process, however its specific role had yet to be addressed.

Recent studies of *fimV* mutants have shown that the lack of T4P assembly is due in part to a defect in secretin formation and the reduced levels of the PilMNOP inner membrane complex (Wehbi et al., 2011). Similar to *pilMNOP* mutants (Ayers et al., 2009), whole cell lysates of *fimV* mutants contained reduced levels of PilQ multimers. When these samples were treated with phenol to dissociate secretins, the overall levels of PilQ monomers in the *fimV* mutants were reduced compared wild type. PilQ overexpression did not compensate for the secretin reduction in *fimV* mutants (Wehbi et al., 2011). This result may indicate a more direct role of FimV in the transitioning of PilQ from its monomer to its multimer states, possibly by allowing PilQ to pass through the peptidoglycan layer to the outer membrane. To support this hypothesis, the LysM domain of FimV was shown to bind peptidoglycan (Wehbi et al, 2011). Further evidence comes from the closely related Type II Secretion System (T2SS) (Peabody et al., 2003; Bitter et al., 1998). ExeAB is a transmembrane heterodimer

that spans the inner membrane of *Aeromonas hydrophila* and is essential for proper function of T2S. ExeAB was shown to be involved in the localization of ExeD (a PilQ orthologue) multimers to the outer membrane (Ast. et al, 2002). The ExeB component interacts with peptidoglycan and was proposed to be involved in its remodelling to allow passage of ExeD to the outer membrane (Howard et al., 2006). As both *A. hydrophila exeAB* and *P. aeruginosa fimV* mutants have an overall reduction in secretin formation, they may play similar roles in their respective systems. However, it is important to note that the presence of the peptidoglycan-binding domain is not sufficient for wild type twitching motility, as demonstrated by the S125 transposon mutant presumably expressing FimV with only a small C-terminal truncation.

1.7 Objectives

Although T4P are found in many bacterial pathogens, we are limited in our understanding of how they function and how they are regulated. Specifically, the role of FimV in the T4P system is not well understood, as there is a lack of biochemical data to explain the observed genetic phenotypes. Through mutational analysis, *fimV* has been identified as an essential gene for twitching motility (Semmler et al., 2000). It is the purpose of this research to provide biochemical data to elucidate the mechanism by which FimV works in *P. aeruginosa* to promote the

function of T4P. Based on our data, we hypothesize that the C-terminal domain of FimV interacts with components of the Pil-Chp chemotaxis system to regulate pilus biogenesis.

2.0 MATERIALS AND METHODS

2.1 Bacterial strains, plasmids and growth conditions

The bacterial strains and plasmids used in this study are listed in Table 1. PAO1 Tn5 Lux transposon mutants were a generous gift from Dr. Robert Hancock, University of British Columbia. These included PAO1_Lux 20_D1, and PAO1_Lux21_F1 (also termed *fimV346* and *fimV2091* with Tn5 Lux insertions in *fimV* at bases 346 and 2091, respectively) (Lewenza et al., 2005). Another transposon mutant, PAO1_*phoA*bp02q3G10 (termed *fimV1129* with a Tn5 IS50L derivative IS*phoA*/hah insertion in *fimV* at base 1129), was obtained from the Manoil laboratory (Jacobs et al., 2003). All bacterial strains were grown at 37°C in liquid cultures in Luria-Bertani (LB) broth or on LB media solidified with 1.0- 1.5% Select agar. Antibiotic selection was as follows, unless otherwise stated: gentamicin 15 mg/L (for *E. coli*) or 30 mg/L (for *P. aeruginosa*) and ampicillin 100 mg/L for *E. coli*.

2.2 Genetic manipulations

P. aeruginosa PAO1 genomic DNA was isolated by using InstaGene Matrix as described by the manufacturer (Bio-Rad). Gene products were amplified by PCR using Hot Start Taq Plus DNA polymerase (Qiagen). Oligonucleotide synthesis and DNA sequencing

were contracted to ACGT DNA Technologies Corporation (Toronto, Ontario, Canada) or Mobix Laboratories (Hamilton, Ontario, Canada). A list of primers used in this study can be found in Table 2. PCR products were purified with the Qiagen gel extraction kit (Qiagen) and plasmids were purified using Qiaprep spin miniprep kit as per the manufacturer's instructions (Qiagen).

2.3 Plasmid transformations

P. aeruginosa strains were transformed with plasmids of interest by electroporation (Dower et al. 1988). A sterile loop full of freshly grown cells were resuspended and washed in 1 mL of nuclease free water and washed 3 times. In the electroporation cuvette, 150 μL of the resuspended cells and 100 ng of plasmid DNA were mixed. The cells were electroporated at a constant 2.5 V while time constants remained above 4 msec. Cells were resuspended in LB for 3 hours at 37°C shaking at 220 RPM to recover. Transformants were then plated on a 1.5% LB agar plate with appropriate selective antibiotics. Resulting colonies were re-streaked and grown over night at 37°C to obtain single colonies.

E. coli strains were transformed by heat shock (Chung et al, 1989). Cells were thawed on ice and incubated with 100 – 200 ng of plasmid DNA for 30 min with gentle mixing. Cells were then immersed in a 42°C water bath for 45 sec and quickly placed back on ice for 15 min. Cells

were resuspended in LB for 3 hr to recover. Cells were then inoculated on a 1.5% LB agar plate with appropriate selective antibiotic. Cells were streaked and grown over night at 37°C for single colonies.

2.4 Site-directed mutagenesis

For mutagenesis of the pFimV6His complementation construct, QuikChange® Site-Directed Mutagenesis technology (Stratagene) was used. Briefly, 5 μL 10x Pfu buffer, 1 μL dNTPs, 125 ng forward and reverse primers (**Table 3**), 100 ng pFimV6His and 1 U Pfu Turbo were mixed to a final volume of 50 μL. A thermocycler was used to denature the template DNA, anneal the complementary primers and elongate the mutated product. Once thermocycling was complete, 1 U of DpnI was added to the 50 μL reaction for 3 hours at 37°C to digest the methylated, unmutated parental strand. Once DpnI reaction complete, 5 μL of the reaction was used heat shock transform the mutated plasmid into *E. coli* DH5α. Single colonies were grown and plasmids were isolated by miniprep (Qiagen). Purified plasmids for sent for sequencing (ACTG) to confirm incorporation of the mutation.

2.5 SDS – PAGE and western blot analysis

Whole cell lysates were made by performing 1/5 dilution of overnight cultures grown in LB with appropriate antibiotics to an $O.D._{600}$ of

0.6, then harvesting the cells from a 1 ml aliquot by centrifugation for 3 min at 16,000 x g. The pellet was resuspended in 100 µL of 1x SDS – PAGE loading dye (125 mM

Tris pH 6.8; 2 % (v/v) 2-mercaptoethanol; 20 % (v/v) glycerol; 0.001 % (w/v) bromophenol blue; 4 % [w/v] SDS). Whole cell lysate and protein samples were boiled for 10 min and 10 µL of the samples were resolved on 12.5% SDS – PAGE gels at 150V. SDS – PAGE gels analyzed by western blot they were transferred to nitrocellulose membranes at 225 mA for 1 hr, otherwise they were visualized with 1% (w/v) Comassie brilliant blue stain (50% (v/v) ethanol and 25% (v/v) acetic acid) by staining for 1 hr at 25 °C and destaining (20% (v/v) ethanol and 10% (v/v) acetic acid) at 25°C until resolved. Membranes were blocked in 5% skimmed milk (w/v) in phosphate buffered saline (PBS, pH 7.4) overnight at 4°C followed by incubation in the appropriate rabbit antisera for 2 hr at 25°C (dilutions of each antisera used are listed in Table 3). After 3 washes in PBS, blots were incubated in goat anti-rabbit IgG AP secondary antibody (Bio-Rad) for 1 hr at 25°C. After 3 washes in PBS, blots were visualized with alkaline phosphatase developing solution containing nitro blue tetrazolium and 5-Bromo-4-chloro-3-indolyl phosphate (Bio- Rad) as per manufacturer's instructions. ImageJ software (NIH) was used to measure and calculate the relative band intensities for quantitative comparative data.

2.6 Twitching motility assays

Twitching motility was tested and measured as previously described (Gallant et al., 1995; Semmler et al., 1999). Briefly, colonies were stab inoculated through 1% agar with a sterile 200 µL pipette tip to the underlying polystyrene Petri dish and incubated at 37°C for 48 hr. The resulting zones of twitching motility were visualized by removing the agar and staining the bacteria adhering to the polystyrene Petri dish with 1% (w/v) crystal violet for 10 min at room temperature, followed by washes with tap water to remove unbound dye. ImageJ software (NIH) was used to measure and calculate the average areas of the resulting twitching zones for quantitative comparative data. Assays were performed in triplicate.

2.7 Analysis of sheared surface proteins

Cell surface appendages were isolated using the methods of Castric (1995) with modifications. Bacteria were streaked in a grid pattern on LB plates with no antibiotics (three plates per sample were used) and incubated overnight at 37°C. Cells were gently scraped off the agar surface with a sterile microscope coverslip and resuspended in 3 mL of sterile phosphate-buffered saline (PBS, pH 7.4) per sample. The surface proteins were sheared by vigorously vortexing for 30 s. The suspension was transferred to two 1.5 mL microcentrifuge tubes and centrifuged for 7

min at 16 000 x g at room temperature to pellet the cells. The supernatant was transferred to new tubes and centrifuged for an additional 30 min at 16 000 x g at room temperature to remove remaining cells. To precipitate the sheared proteins, 1/10 volume of each 5 M NaCl and 30% polyethylene glycol (MW range 8000), was added to the supernatant and the samples were incubated on ice for 60 min. Samples were centrifuged at 16 000 x g at 4°C for 25 min and the supernatant was discarded. Samples were centrifuged for an additional 7 min to remove residual fluid. The resulting pellets were resuspended in 1x SDS-PAGE loading dye (125 mM Tris, pH 6.8; 2% (w/v) 2-mercaptoethanol; 20 % (v/v) glycerol; 0.001% (w/v) bromophenol blue; 4% (w/v) SDS), boiled for 10 min and resolved on a 15% SDS-PAGE gel with a pre-stained Benchmark Protein Ladder (Invitrogen). The proteins were visualized using Coomassie Blue dye or analyzed by western blot.

2.8 Generation of *6xhis – fimV* expression constructs

All *pET151* constructs were generated using TOPO isomerase cloning technologies (Invitrogen). Specifically, following PCR amplification of the gene of interest and amplicon purification, 4 μL of the gel extracted amplicon was incubated with 1 μL of the TOPO vector, and 1 μL of the salt buffer solution provided to a final volume of 6 μL. The cloning reaction was left incubating at 25°C for 5 min. *E. coli* TOP10 cells were then heat

shot transformed with 3 μL of the cloning reaction. Single colonies were streaked on 1.5% LB agar plates for dense bacteria growth to harvest carrying plasmids. Restriction digest using XbaI and SacI was used to visualize amplicon drop out and determine amplicon insertion into the plasmid. Plasmids containing amplicon were sent for sequencing to ensure gene accuracy.

2.9 Large – scale protein expression from the *pET151* plasmid

E. coli BL21 was transformed with the expression construct. Single colonies following the heat shock transformation were used to inoculate 10 mL of LB ampicillin 100 mg/L for overnight culture at 37°C. The 10 mL overnight was subcultured into 1 L LB ampicillin 100 mg/L at 37°C, shaking at 200 – 225 RPM. Gene expression was induced with 1 mM IPTG (Sigma) once cells reached an O.D. of 0.4 – 0.6. Induction of cells would continue for 3 – 4 hrs. Cells were then harvested by centrifugation at 3,200 x g and flash frozen in liquid nitrogen and stored at -80°C until required. Induced and uninduced samples were taken for SDS PAGE and western blot analysis.

2.10 Protein purification

Harvested cell pellets were thawed on ice and resuspended in 20 mL of lysis buffer containing 500 mM KCl, 0.1% lauryldimethylamine-oxide

(LDAO), 100 mg/L RNase, 100 mg/L DNase, 100 mg/L benzamidine, and 20 mM Tris pH 8. The mixture was then sonicated on ice with alternating 10 sec on and 15 sec off periods for a total on time of 5 min. Lysates were clarified by centrifugation at 48,000 x g to separate soluble and insoluble materials.

The clarified lysate was applied to a 5 mL Nickel column (Amersham), pre-equilibrated with Ni A buffer containing 10 mM imidazole, 500 mM KCl and 20 mM Tris pH 8. The flowthrough fraction as well as 20 mL washes containing 10 mM, 20 mM, 40 mM concentrations of imidazole were collected. The protein was eluted with 30 mL of a Ni B buffer containing 75 mM imidazole 500 mM KCl and 20 mM Tris pH 8. The eluted fraction was promptly dialyzed overnight at 4°C into a buffer containing 0 – 200 mM KCl and 20 mM Tris pH 6 – 8.

Size exclusion chromatography was conducted to further purify proteins following nickel chromatography. A Superdex 200 (S200) column was equilibrated with the dialysis buffer. The protein sample was concentrated to a final volume of 200 – 1000 μL and injected onto the S200 column. The elution from the column was monitored by UV absorbance and fractions corresponding to peaks on the chromatogram were collected for SDS – PAGE and western blot analysis.

2.11 Determination of protein concentrations

Protein concentrations were measured with the NanoDrop spectrophotometer ND-1000, using the 280 nm setting and providing the protein theoretical extinction coefficient and molecular weight from Expasy Tools software ProtParam (http://web.expasy.org/protparam/). To verify the NanoDrop calculations, bicinchoninic acid (BCA) assays (Pierce) were performed. Briefly, using a 96 well plate, reagents A and B were mixed in a 1:50 ratio to a final volume of 200 μL and equilibrated for 5 min as per manufacturer's instructions. Once equilibrated, 25 μL of BSA standards were added to the wells containing the mixtures. The protein sample of unknown concentration was also added to the wells with the reagent AB mixtures and allowed to equilibrate for 15 min at 37°C shaking at 50 rpm. The absorbance at 600 nm was determined, and a standard curve was constructed using the BSA standards. All of the readings were performed in triplicate.

2.12 TEV proteolysis

Where indicated, TEV proteolysis was used to cleave the 6xHis and V-5 epitope tags following nickel chromatography purification and dialysis. The purified protein was incubated with 1 mg of purified TEV protease at 25°C for 2.5 hrs. The reaction was terminated with the addition of benzamidine to a final concentration of 100 mg/L. The reaction mixture

was then applied to a pre-equilibrated 5 mL nickel column (Amersham) and the flowthrough containing the protein of interest was collected and dialyzed into a buffer containing 0 – 200 mM KCl and Tris pH 6 – 8.

2.13 Circular dichroism spectroscopy

Purified protein was dialyzed into PBS buffer prior to performing circular dichroism (CD) spectroscopy. Unless stated otherwise, protein samples were adjusted to a final concentration of 0.5 mg/mL prior to the assay. In the case where protein samples were mixed, incubation was at 4°C overnight. Absorbance was measured at intervals of 1 nm from 190 nm to 260 nm, with a data collection time of 5 s. The temperature of the sample chamber was set to 25°C. Absorbance values were transferred to Microsoft Excel where the data was normalized and converted to molar elipticity [θ] using the following formula:

[θ]=(Absorbance/1000)/[(Concentration (mg/mL)/Molecular Mass (Da)/1000)x #Amino acids]

2.14 Co-affinity purification assay

Co-affinity purification of 6xHis-tagged FimV was performed to determine interaction partners (Rual et al.,2005). Briefly, PAO1 was streaked out on 1 – 1.5% LB agar plates in a grid-like fashion and allowed to grow over night at 37°C. The bacterial cells were harvested by scraping

with a sterile cover slip and resuspended in PBS containing 100 mg/L benzamidine. The cells were sonicated on ice with alternating 10 s on and 15 s off periods for a total on time of 5 min. The cell lysates were centrifuged for 15 min at 3000 x g to separate unlysed cells from the sonicated mixture. The supernatant was mixed with 10 mg of purified bait protein at 4°C overnight. The mixture was then applied to a pre-equilibrated 5 mL nickel column and the flow-through was collected. Following a 20 mL wash step containing PBS and 10 mM imidazole, the proteins were eluted with 20 mL PBS and 75 mM imidazole. All fractions were collected for SDS – PAGE and western blot analysis.

2.15 Crystallography

Crystal trays were set using the hanging drop / vapor diffusion method (Fowlis, 1988). For initial screening, purified protein at various concentrations and buffer conditions and precipitant solution were mixed in a 1:1 ratio to a final volume of 1 μL. The drops were incubated over a 1.5 M ammonium sulfate solution in a sealed environment at 4 – 30°C, and were regularly checked for crystal formation. Drops were analyzed with a bi-focal light microscope, inspecting for crystal growth conditions. The crystal screens primarily used were the Classics (Qiagen), the JCSG suits I – IV (Qiagen), the PEGS (Qiagen), pH Clear (Qiagen), pHAT (Hampton) and the Wizards I + II (Emerald).

2.16 Peptidoglycan isolation

Peptidoglycan (PG) from *P. aeruginosa* PAO1 was isolated using a boiling SDS protocol and purified by enzyme treatment with amylase, DNase, RNase, and pronase (Clarke, 1993). From 2 liters of overnight growth in LB, cells were collected, washed with 0.5x volume of 50 mM sodium phosphate, pH 7.0, and resuspended in a final volume of 50 ml of the same buffer. The resuspended cells were added dropwise to 50 ml of boiling 8% SDS in 50 mM sodium phosphate, pH 7.0 (4% SDS final concentration), and the mixture was subjected to reflux for 1 hr. PG was collected by ultracentrifugation for 1 hr at 100,000 x g (Beckman Coulter Optima Max-E Ultracentrifuge) and then washed 4 times with buffer to remove SDS. The final PG pellet was resuspended in 10 ml of 10 mM Tris-HCl, 10 mM NaCl with sonication for 1 min. PG was then incubated for 2 hr at 37°C with amylase (100 μg/ml final concentration), imidazole (0.32 M final concentration), DNase I (10 μg/ml final concentration), RNase (50 μg/ml final concentration), and $MgSO_4$ (20 mM final concentration). The PG was then incubated for 2 h at 60°C with preheated pronase (200 μg/ml final concentration). The enzymatically purified PG was then added dropwise to 10 ml 8% boiling SDS in 50 mM sodium phosphate, pH 7.0, and refluxed and washed as before, with the final

wash with dH_2O. The final pellet of purified PG was resuspended in 1 mL water and lyophilized.

2.17 Peptidoglycan pulldown assay

One mg of lyophilized PG was resuspended in 1 ml of 50 mM Tris-HCl, pH 7.0, with sonication for 30 to 45 sec and used as a stock for PG protein binding assays (Scheurwater et al., 2008). Briefly, 15 μg of purified protein was incubated with 150 μL of the 1 mg/ml PG stock (0.15 mg PG final concentration) in a total reaction volume of 300 μL with 50 mM Tris-HCl. A control reaction lacking PG was done concurrently ("initial" fraction). Reaction mixtures were incubated for 2 hr at 4°C with gentle agitation and then centrifuged at maximum speed in a microcentrifuge for 30 min at 4°C. The supernatant containing unbound protein was removed and mixed with 3x SDS sample buffer for analysis. The pellet, containing PG and bound protein, was washed with 300 μL of 50 mM Tris-HCl, pH 7.0, and recentrifuged. The wash supernatant was collected and mixed with 3x SDS sample buffer. To separate protein bound to the PG, the pellet was treated with 300 μL of 4% SDS in 50 mM Tris-HCl, pH 7.0, for 15 min at 4°C and then centrifuged as before. The supernatant containing released protein was collected and mixed with 3x SDS sample buffer. Samples were analyzed by western blotting using anti-His anti-body.

2.18 Fluorescence Microscopy

Fluorescence microscopy of bacteria was performed as described by Chiang et al., 2005. All bacterial strains carrying various YFP constructs were grown in LB gentamicin 30 mg/L at 37°C overnight. Cells were resuspended in 5 µL of sterile PBS and 2 µL of this mixture was fixed on a sterile microscope slide with 2 µL of Cygel (Biostatus Limited, United Kingdom). Cells were visualized on wide-field microscope (Leica DMI 6000 B at 100 x magnification, Hamamatsu Orca Camera, oil immersion lens) using the 472/530 nm filter set.

2.19 Partial Proteolysis

Partial proteolysis was conducted on nickel purified FimV487 as described by Cleveland et al., 1977. Purified FimV487 was concentrated to 10 mg/mL and incubated with trypsin at temperatures of 4°C and 25°C for 15 min, 30 min, 45 min, and 60 min. The concentration of trypsin used ranged from to 0.5 ng/mL to 0.5 mg/mL. The reaction was halted by the addition of 5x SDS sample buffer. Degradation products were analyzed by SDS-PAGE.

3.0 RESULTS

3.1 Bioinformatic analysis of the cytoplasmic region of FimV predicts two tetratricopeptide repeat (TPR) motifs.

The cytoplasmic region of FimV was previous implicated by Semmler et al. (2000) to be crucial for T4P function. To investigate the function of the C-terminal region, secondary structure and protein fold prediction algorithms were used to gain structural information. The cytoplasmic portion of FimV was predicted to be composed of two α-helical regions from residues 487-638 and 862-919 (**Figure 3A).** Psipred (http://bioinf.cs.ucl.ac.uk/psipred/), Jpred (http://www.compbio.dundee.ac.uk/www-jpred/) and PHYRE (http://www.sbg.bio.ic.ac.uk/~phyre/) software each predicted 6-7 α-helices in the first α-helical region and 3 α-helices in the second α-helical region with high confidence E-values of 9.9e-12. PHYRE software modeled the three-dimensional fold of these regions based on amino acid similarity and secondary structure similarity to existing structures. The models in **Figure 3B** are amino acid residues 487-638 and 862-919 threaded onto the nearest matches, a synthetic consensus TPR protein and Cyclophilin 40 (*Bos taurus)* respectively. Both contain the tetratricopeptide repeat (TPR) motif, each of which is a consensus 34

amino acid sequence forming two α-helices joined by a short loop (Mittl et al., 2007). TPR proteins generally have multiple repeats that fold into a superhelix. The residues 487-638 and 862-919 will be designated as TPR1 and TPR2 respectively.

3.2 The cytoplasmic region of FimV displays a circular dichroism absorbance spectra characteristic of α-helical proteins.

To support the bioinformatic data, circular dichroism (CD) was conducted to experimentally determine the potential secondary structure of the cytoplasmic regions of FimV. Expression constructs encoding FimV487-919, FimV487-634 and FimV862-919 were generated as described in the METHODS section and products of these constructs are modeled in **Figure 2C**. Following 1L expression of these proteins, the FimV fragments were purified using nickel chromatography and eluted in 55 mM imidazole fraction as visualized by the SDS – PAGE analysis (**Figure 4 A – C).** The FimV fragments migrated in the SDS-PAGE gels according to their expected molecular weights, with the exception of FimV487 and FimV634. It was previously noted by Semmler et al. (2000) that FimV has aberrant migration in SDS–PAGE analysis. A typical yield from a 1 L culture preparation was approximately 20 mg/mL, as determined by both protein absorbance at 280 nm with the NanoDrop and a BCA assay (data not shown).

The purified protein fragments were then analyzed using CD spectroscopy. The samples were diluted to 0.5 mg/mL prior to analysis. As predicted by the bioinformatic software, FimV635 and FimV862 gave CD spectra characteristic of α-helical proteins (**Figure 5)**. The molar ellipticity of FimV862 was calculated to be -16000 θ at both 208 and 222 nm. FimV632 had molar ellipticity values of -8900 θ and -8100 θ at 208 and 222 nm respectively. FimV487 also had an α-helical CD signature with its higher wavelength local minima at 222 nm calculated at -6500 θ, however, with its local minima blue-shifted to 206 nm with a value of -10000 θ as seen in **Figure 5 C)**. This spectra is characteristic of a protein with a mixture of random coil and α-helices (Provencher et al., 1981).

3.3 FimV co-purifies with the inner membrane complex member PilM and the chemotaxis protein PilG.

TPR motifs have been characterized as protein-protein interactions sites (Mittl, 2007). A co-affinity nickel chromatography experiment was performed to determine if interaction partners of FimV could be identified. Both FimV487 and FimV862 contain an N-terminal 6xHis tag that was used to immobilize the proteins to the charged nickel resin. FimV487 and FimV862 were purified with the affinity tag (**Figure 4)**, prior to the co-purification experiment. When FimV487—which contains both TPR1 and TPR2—was incubated with the whole cell lysate of PAO1, both PilG and

PilM co-eluted with FimV487 in the 55 mM imidazole elution step (**Figure 6A and 6B**). As controls, neither PilH or PilO co-eluted with FimV487 (**Figure 6 C and 6D).** Other assembly proteins including PilN, PilP, PilB, PilU, PilT were not present in the final elution (data not shown). When FimV862—which contains only TPR2—was incubated with PAO1 whole cell lysates, only PilM was detected in the final elution. In the absence of FimV fragments, no proteins were identified in the final elution step (**Figure 6 E).**

3.4 FimV gains some α-helical structure upon incubation with PilG.

Based on the bioinformatic analysis in **Figure 3A** and supporting CD data in **Figure 5C**, the fold of FimV 635 – 861 is mostly unstructured. It has been noted that unstructured regions may gain structure upon binding to their interaction partners (Koag et al., 2003). Because FimV487 contains a flexible, unstructured region, potential structural changes in FimV upon interaction with PilG were analyzed by incubating purified FimV487 with purified PilG at molar ratios ranging from 3:1 to 1:6 of FimV:PilG. CD spectroscopy was conducted on these samples, using FimV487 mixed with PilH as a negative control and PilH and PilG alone as background absorbance controls. The spectra of PilH and PilG were subtracted from the spectra of the mixed samples to detect the spectrum of FimV487 in the mixed state.

The CD spectra of purified PilG is characteristic of a mixture of secondary structural elements of α-helices and β-strands, however the overall calculated molar ellipticity is very weak, as local minima are 2250 θ and 3000 θ (**Figure 7A**). **Figure 5C** shows the spectrum for FimV487 alone. When FimV487 was incubated overnight with PilG, the molar elipticity of FimV487 increased in magnitude by 10%, as local minima values at 222 nm and 206 nm decrease from -6500 θ and -10000 θ to 7000 θ and 11000 θ respectively. These new molar ellipticity values are more α-helical than those of FimV487 alone. When FimV487 was incubated with PilH over night in a 1:3 molar ratio of FimV487:PilH, no change in FimV487 molar ellipticity was observed.

3.5 *fimV and pilG* mutants have reduced levels of the inner membrane complex proteins PilMNOP.

Previously, Wehbi et al (2011) showed a reduction in the levels of the inner membrane complex proteins PilMNOP in the *fimV346* mutant. These reduced levels may be caused in part by a reduction in the intracellular levels of cAMP in the *fimV* mutant (Fulcher et al., 2010) due to regulation of the *pilMNOP* operon by the cAMP-binding protein, Vfr (Kanack et al., 2006). Fulcher et al. (2010) also showed that *pilG* mutants had reduced levels of cAMP. To examine the effect of PilG on PilMNOP levels, intracellular levels were measured by western blotting.

Levels of PilM/N/O/P in a *pilG* mutant were 67%, 55%, 46% and 46% of wild type, respectively (**Figure 8**). This reduction is comparable to the reduction seen in the *fimV346* mutant, where PilM/N/O/P levels are 86%, 68%, 45%, and 27% to that of wild type respectively. When the *pilG* mutant was complemented *in trans* with a pUCP20Gm:*pilG* plasmid, levels were restored to close to or above wild type levels.

3.6 PilG is mis-localized in the *fimV* mutant.

It was previously shown by H. Khalil (M.Sc. thesis, 2010) that PilG is localized to the poles of the cell. This localization pattern may have a functional role in allowing PilG to act on the T4P system or on the CyaB adenylate cyclase, which is also polar (Inclan et al., 2011). How PilG is localized to the pole is not, however, well understood. Using a complementation construct encoding a PilG-YFP fusion protein, PilG localization was examined in *P. aeruginosa* mutant strains using fluorescent microscopy (**Figure 9). Table 4** summarizes the strains used and their PilG localization phenotype**.** The PilG-YFP expression construct was previously shown to be functional, as complementation of a *pilG* mutant with this construct restored twitching motility (H. Khalil M.Sc. thesis, 2010). Panels **A – D** are fluorescent microscopy images of WT, *pilG, fimV346 and cyaAB* mutants expressing YFP. There does not appear to be any preferential sub-cellular localization of YFP. In panel **E**

and **F,** PilG-YFP was expressed in both WT and *pilG* respectively. Punctate fluorescence was observed at the poles of the cells. In the *fimV346* mutant expressing PilG-YFP, only a diffuse localization was observed (panel **G).** In panel **H,** a *cyaAB* mutant expressing PilG-YFP displayed wild type localization of PilG. When PilG-YFP was observed in *fimV2091, fimV1194* and *pilH,* PilG localization was diffuse as well. Interestingly, in *E. coli* DH5α PilG-YFP had a diffuse localization pattern (**Table 4**).

4.0 ADDITIONAL RESULTS

4.1 The LysM domain of FimV binds peptidoglycan

Semmler et al. (2000) reported the presence of a putative LysM domain in the periplasmic region of FimV. The LysM domain is commonly associated with peptidoglycan interactions (Buist et al., 2008). To test whether FimV interacts with peptidoglycan, three periplasmic fragments of FimV (FimV129, FimV254 and FimV390) were purified (**Figure 4D).** As described in the METHODS section, these three fragments were incubated with peptidoglycan isolated from PAO1 and a PG pulldown down assay was conducted. FimV129, which does not contain the LysM domain, was found in the unbound fraction, whereas FimV254 and FimV390, which contain the LysM domain, appeared in the bound fraction. The samples were analyzed by a western blot using monoclonal antibodies against 6xHis (**Figure 10)**. There is a greater band intensity in the FimV390 bound fraction compared to FimV254, as the pFimV390 construct encodes two 6xHis-tags whereas pFimV254 encodes one.

5.0 RESULTS IN PROGRESS

5.1 Crystallography of FimV

FimV254, FimV487, FimV634 and FimV862 were expressed and purified using nickel chromatography (**Figure 4).** FimV254 was screened for protein crystallization at concentrations from 2 mg/mL to 25 mg/mL using the Classics and Wizards screens (Fowlis, 1988). No protein crystals were obtained from these screens. FimV634 was screened at concentrations of 20 mg/mL and 40 mg/mL. The Classics, Wizards, and JCSG suites I-IV were used to screen for protein crystallization however no protein crystals have formed at this time. After days of incubation, most conditions remained clear and less than 1% of the conditions tested caused the protein to precipitate. Phase separation was frequently observed, however no noticeable correlation with the buffer conditions was observed.

Most of the effort of the crystallography project was directed to crystallizing FimV487, as it contained the full cytoplasmic region of FimV. FimV487 was further purified by gel filtration prior to using crystal screens (**Figure 11**). Fractions collected from the first peak after the void volume were pooled and concentrated to 5 mg/mL to 60 mg/mL. The screens used were the Classics, JCSG suites I-IV, Wizards, Crystal Magic, pHClear, pHAT, the PEGS and the Cation Suite. After screening many

salt crystals, no protein crystals of this protein fragment were obtained. As with FimV634, but very few conditions caused FimV487 to precipitate and phase separation was frequently observed.

Following nickel chromatography purification and TEV proteolysis (**Figure 4A)**, FimV862 was concentrated and crystal trays were set at a protein concentration of 4 mg/mL. The Classics crystal screen was used and protein crystals were observed in a condition containing 50 mM KCl, 250 mM NaCl, 50 mM tri-sodium citrate pH 5.6, and 2% (v/v) ethylene imine polymer (**Figure 12A**). X-ray diffraction patterns were collected for the protein crystals (**Figure 12B**) and diffraction spots correlating to 3.4 Å resolution were obtained (data not shown). Based on the crystal morphology and diffraction pattern data, further optimization of the crystals is required to obtain single crystals as the current crystals are twinned.

5.2 Characterization of stable fragments of FimV and FimV/PilG interactions by partial proteolysis.

To identify key regions of FimV that may be involved in the interaction with PilG, a partial proteolysis experiment was initiated. In a partial proteolysis experiment, if a residue that can be cleaved by a protease is exposed, the protease will cleave at that residue, producing degradation products. If, however, a target residue is not exposed due to the fold of the protein or if the target residue is buried within a protein-

protein interface, the protease will not be able access the residue and degradation will be limited (Cleveland et al, 1977). In this experiment, structural regions of FimV as well as any possible insights as to any key residues or region of FimV that are involved in the interaction with PilG were examined by trypsin digest. **Figure 13** shows the control experiment that is meant to establish the conditions most suitable for the FimV-PilG partial proteolysis experiment. Suitable conditions would show a range of degradation products that could be tracked based on protease concentration and incubation time. As seen in **Figure 13**, a trypsin digest using purified FimV concentrated to 10 mg/mL was conducted at time points of 15 min, 30 min, 45 min and 60 min at concentrations of trypsin ranging from 0.5 mg/mL to 0.5 ng/mL. At an incubation period of 15 min and trypsin concentration of 50 μg/mL, several degradation products ranging from 10 to 55 kDa were visualized by SDS – PAGE analysis. There was also a unique, intense band at 26 kDa in the lanes where 50 μg/mL of trypsin was used. This condition may be suitable to examine the interaction between FimV and PilG.

6.0 DISCUSSION AND FUTURE DIRECTIONS

The importance of *fimV* to T4P function was previously demonstrated by mutant analyses (Semmler et al., 2000). However, the specific function of the *fimV* gene product remains enigmatic. FimV was proposed to have some role in peptidoglycan interaction with the identification of the LysM domain in the N-terminal region of the protein (Semmler et al., 2000). Evidence to support this hypothesis was provided by demonstrating that FimV interacts with peptidoglycan, and by showing the importance of its LysM domain for secretin formation (Wehbi et al., 2011). But the LysM domain was not the only important feature of FimV for functional T4P. A transposon insertion in last 30 base pairs of the *fimV* gene was presumed to produce a truncated gene product that resulted in aberrant twitching phenotypes (Semmler et al., 2000). This result implicated the C-terminal region of FimV as having an important role in twitching motility as well. This result was further supported by data showing that both halves of FimV (the full cytoplasmic region and the full periplasmic region) expressed *in trans* are necessary to restore twitching motility in a mutant lacking FimV (Wehbi et al., 2011). The expression level of FimV must also be tightly regulated, as over-expression of the gene was reported to block twitching motility (Semmler et al., 2000). Based the findings in this study, we demonstrated that the C-terminal region of FimV is an important component who's function is involved in the

regulation of the T4P system, through the interactions with other proteins in the system.

6.1 Bioinformatic analysis of FimV reveals TPR protein-protein interaction motifs

Secondary structure recognition software predicts the cytoplasmic portion of FimV to be mostly α-helical in nature, with two α-helical regions separated by a long stretch of unstructured amino acids (**Figure 3A**). PHYRE analysis suggested that the two α-helical segments were tetratricopeptide repeat (TPR) motifs. TPR motifs are alpha helix-turn-helix-turn repeats of 34 amino acids that form a superhelical structure when arranged in succession, and are typically involved in protein-protein interactions (Magliery and Regan, 2004; Mittl and Schneider-Brachert, 2006; Main et al., 2003). This predicted structure for the C-terminus of FimV is supported by the CD data in this study that shows the C-terminus is highly α-helical. Interestingly, another protein in the T4P system, PilF, is made up entirely of TPR motifs. PilF has been linked to protein-protein interactions with the secretin, PilQ (Koo et al., 2009). These predicted TPR domains in FimV have also been shown in this study to interact with PilG and PilM. Although the PHYRE prediction of the cytoplasmic portion of FimV models an odd number of α-helices, secondary structure

prediction shows there are more α-helices that are not modeled, perhaps due to poor homology.

6.2 FimV-PilG interaction may be direct or indirect

From the co-purification assay it was unclear whether TPR2 was required at all for PilG binding, however evidence to support that TPR2 may be involved in interacting with PilG comes from PilG localization data, as PilG is still diffusely localized in the *fimV2091* strain (**Table 4**), as *fimV2091* still produces most of the FimV protein except TPR2. It is possible however that the expression product of the *fimV2091* mutant may not be sufficiently folded for interaction with PilG. From the localization and co-purification data, it is unclear what role the unstructured region has in the FimV-PilG interaction and whether these interactions are direct or indirect interactions. Notably, there are a few bands in a Coomassie stained SDS-PAGE gel of the eluted fraction of the co-purification assay (data not shown). It is important to have those bands analyzed by mass spectrometry to find out what else may be interacting with FimV. To determine whether these proteins are directly interacting, FimV487 and PilG could be purified separately and co-elution on a gel filtration column would suggest a complex formation. The CD data in **Figure 7** does support the hypothesis that the two proteins interact directly, but it is unclear based on the modest shift observed whether the unstructured

region is gaining structure, or if the α-helical TPR1 is undergoing a slight conformational change that increases the α-helical signal. It is not believed that the change in viscosity is the cause for the shift since the molar elipticity is unchanged at varying concentrations of FimV. Nonetheless, a modest conformational change in FimV is observed. A partial proteolysis experiment may also show that FimV and PilG are directly interacting. If upon binding, PilG hides a region of FimV that is typically cleaved by a protease as seen in **Figure 13**, fewer FimV degradation products would be observed on an SDS-PAGE gel. This experiment would not only demonstrate their direct interaction, but also a key surface of FimV that is involved in the interaction.

6.3 FimV may be important for T4P polar localization

The significance of the FimV-PilM interaction is not entirely clear. PilM is a cytoplasmic protein with an actin-like fold (Martin et al., 1995) very similar to that of FtsA, a protein involved in cell division (Lara et al., 2005). It is possible that PilM is important for shuttling components of the T4P to the pole of the cell during cell division as the pole is being newly formed from the septum. This hypothesis is consistent with the data that demonstrates the importance of FimV in secretin formation and the peptidoglycan binding nature of FimV (Wehbi et al. 2011). If FimV is localized to the septum of the cell by PilM, it can bind to peptidoglycan

while it is being formed and maintain gaps, allowing for PilF to shuttle PilQ monomers to the outer membrane.

6.4 FimV may regulate T4P through interactions with the chemotaxis protein PilG

PilG is a response regulator protein encoded in the *pil-chp* chemotaxis gene cluster. This chemotaxis system is modeled from the *E. coli* chemotaxis system that regulates the direction of the rotation of the flagellum, ultimately dictating the direction of the bacteria's translocation. The T4P associated chemotaxis system is believed to sense an extracellular signal which relays a signal though the chemotaxis complex to the T4P assembly complex. The specific extracellular signal(s) and the mechanism by which the chemotaxis system may influence T4P function are not known. PilG has been linked to twitching motility in many studies and *pilG* mutants have been shown to have pilus assembly defects (Khalil M.Sc. thesis).

Recently, *fimV* and *pilG* mutants have been shown to have reduced levels of intracellular cAMP (Fulcher et al., 2010). cAMP is an important molecule in the regulation of many *Pseudomonas* virulence factors, including T4P as it binds to Vfr (virulence factor regulator) (Kanack et al., 2004). Vfr is a homolog of *E. coli's* well-studied CRP and is a transcriptional regulator of many of virulent genes. Vfr has been shown to

regulate the transcription of the *pilMNOPQ* operon upon binding to cAMP. The reason as to why cAMP levels are reduced in these mutants is not well understood. In the *fimV and pilG* mutants, there is no significant reduction in the adenylate cyclases CyaA or CyaB that make cAMP from AMP, the only two adenlate cyclases found in *Pseudomonas*, or Vfr (Fulcher et al., 2010). Based on these results, it is believed that PilG and FimV may somehow be affecting CyaAB activity. CyaB was previously shown to localize to the poles of the cell (Inclan et al., 2011). In this study, we have shown that FimV affects the localization of PilG. We hypothesize that *pilG* and *fimV* mutants affect CyaB activity because of the absence of PilG at the pole of the cell.

In the studies conducted by Wehbi et al., 2011, reduced levels of intracellular PilMNOPQ were reported however the connection between FimV and cAMP was not known at the time of the submitted publication. We hypothesized that since cAMP levels are reduced in a *pilG* mutant, the expression levels of the inner membrane complex PilMNOP should be comparably reduced compared to the *fimV* mutant. We observed a reduction in all of gene products of the *pilMNOP* operon and were able to restore the protein levels back to wild type levels by complementing the *pilG* mutant with a plasmid expressing the PilG protein *in trans.* Based on these results and those of previous studies, the assembly defects in a *pilG* mutant is due to the reduction of cAMP and consequently the reduced

levels of PilMNOP as complementation of a *pilG* strain with exogenous cAMP restores pilus assembly (Fulcher et al., 2010; Ayers et al., 2009).

6.5 FimV structural studies

To help determine the function FimV, x-ray crystallography was attempted to obtain the 3D structure of the protein. Unfortunately, no viable protein crystals have been obtained that can used for structure determination. Crystallization of the cytoplasmic region of FimV would prove to be difficult due to the acidic nature of the protein. The protein is very negatively charged at neutral pH, so the protein is exceedingly soluble. This solubility is an issue, as the protein needs to come out of solution to form protein crystals (Asherie 2004). Another reason for the difficulty of this protein to nucleate is the electrostatic repulsion due to its overall negative charge. Attempts to neutralize the negative charge were made by lower the buffer pH and quenching the negative charge with cationic salt screens however only limited success has been seen. Crystallization of FimV487 would appear to be even more difficult due to the unstructured coiled region separating the two predicted TPR motifs. Partial proteolysis of FimV487 has be conducted to map out the more highly structured regions of FimV, which may prove useful for *in situ* proteolysis for protein crystallization (Dong et al., 2007).

The only protein crystals obtained came from screening purified FimV862 and the crystal diffracted with a resolution of 3.4 Å. Unfortunately the protein crystal requires further optimization due to the crystal twinning. Iterative seeding or an additive screen may produce single crystals suitable for x-ray diffraction data collection. Protein NMR is a viable alternative method for structure determination, specifically for FimV862 as its small size makes it a good candidate for NMR (Montelione et al 2000).

7.0 CONCLUSIONS AND SIGNIFICANCE

It was previously reported that *fimV* was an essential gene, important for the assembly of T4P, however, how FimV functions within the T4P system was not known (Semmler et al, 2000). It was hypothesized that FimV may have some role in binding peptidoglycan based on bioinformatic analyses that identified a LysM motif in the periplasmic region of FimV. We have since provided evidence supporting the hypothesized role of the N-terminus of FimV in peptidoglycan interactions and the importance of such interactions in secretin formation (Wehbi et al, 2011). The importance of the cytoplasmic region of FimV was first suggested by Semmler et al. 2000 when they showed even a small trunctation of the C-terminal end of the FimV protein had an aberrant twitching phenotype. The study by Fulcher et al. 2010 suggested a role for the cytoplasmic region of FimV in cAMP regulation, similar to components encoded by the *pil-chp* gene cluster. In this work, we provided evidence explaining the connection between these components, showing that FimV interacts with and localizes the key response regulator PilG, to regulate twitching motility and other virulence factors of *P. aeruginosa* regulated by Vfr (**Figure 1**). Fulcher et al. 2010 suggested that PilG may be directly influencing the activity of CyaB. In this study, it was demonstrated that FimV is important for PilG localization. It was also

previously shown that CyaB is polarly localized (Inclan et al., 2011). We hypothesize that the presence of PilG is not enough for CyaB activity, but PilG must also be properly localized. By identifying interaction partners of FimV, we will have a clearer understanding of its role in the T4P complex as well as a more accurate picture of T4P complex function. These findings are necessary for the rational design of strategies to impede pilus-related virulence.

8.0 APPENDIX

8.1 Suplementary Data

8.1.1 Complementation of *fimV* mutants with pFimV

As noted in **Table 1** and **Figure 1**, there are a variety of *fimV* mutants, each with different expression products. These expression products were analyzed by western blot analysis with polyclonal antibodies raised against the C-terminal and N-terminal regions of FimV (E. Portillo M.Sc. thesis, 2009). Complementation of these strains using the pFimV6His complementation construct yielded different twitching phenotypes and have levels of recoverable surface pili. It was proposed that the 6xHis-tag was having some affect on the observed phenotypes as complemented strains that express only C-terminal domains of FimV that contain the 6xHis-tag (*fimV346* + pFimVHis and *fimV2091* + pFimVHis) twitch well above wild type levels and lower levels of recoverable pili, whereas strains that still express endogenous C-terminal domains (WT and *fimV1194*) have wild type phenotypes (Portillo M.Sc. thesis). This hypothesis was tested by introducing a stop codon into the pFimV6His construct just before the first histidine codon. This construct was then termed pFimV. The twitching zones and surface pilin of WT, *fimV1194, fimV346 and fimV2091* were compared when complemented with both pFimV and pFimV6His. No significant difference in the size of twitching

zones (**Figure 14 A**) and levels of surface pilin (**Figure 14 B**) were observed when complemented with either pFimV or pFimV6His, however between some strains there were a significant differences. There were no significant differences between *fimV2091* and *fimV346* or WT and *fimV1194* as previously reported (Portillo M.Sc. thesis). The different phenotypes may have been a result of where the strain originated. As noted in **Figure 14 A)**, WT was received by Jacobs et al., 2003 and the *fimV1194* mutant was made from this WT strain, however, *fimV346* and *fimV2091* were received by Lewenza et al., 2005.

8.2 Tables and Figures

Table 1. List of bacterial strains used in study

Strain or Plasmid	Relevant Characteristics	Source or reference
E. coli		
***E. coli*DH5α**	F- *φ80lacZΔM15 Δ(lacZYA-argF)*U169 *recA1 endA1 hsdR17(rk-, mk+)phoAsupE44 thi-1 gyrA96 relA1 λ-*	Invitrogen
***E. coli*TOP10**	F-*mcrAΔ(mrr-hsdRMS-mcrBC)φ80lacZΔM15 ΔlacX74 recA1 araD139 Δ(araleu)7697 galUgalKrpsL (StrR) endA1 nupG*	Invitrogen
***E. coli*BL21(DE3)**	F– *ompT hsdSB(rB–, mB–) gal dcm rne131 (DE3)*	Invitrogen
***E. coli*DH5α + pMarkiN**	DH5α strain carrying pUCP20Gm:*yfp*	This study

***E. coli*DH5α + pMarkiC:pilG**	DH5α strain carrying pUCP20Gm:*pilG-yfp*	This study
P. aeruginosa		
PAO1	Wild-type; piliated, twitching	Jacobs et al, 2003
PAK	Wild-type; piliated, twitching	Fulcher et al., 2010
PAO1 NP	Transposon mutant, Tn5 *ISphoA/hah* insertion in *pilA* at base 163; non-piliatedal (NP), no twitching	Jacobs et al, 2003
PAO1 *pilM*	PAO1 with SmaI-flanked FRT insertion at position 529 (Eco47III) in *pilM*	Wehbi et al, 2011
PAO1 *pilN*	PAO1 with SmaI-flanked FRT insertion at position 124 (ScaI) in *pilN*	Wehbi et al, 2011
PAO1 *pilO*	PAO1 with SmaI-flanked FRT	Wehbi et al,

	insertion at position 42 (EcoRV) in *pilO*	2011
PAO1 *pilP*	PAO1 with SmaI-flanked FRT insertion at position 86 (ScaI) in pilP	Wehbi et al, 2011
PAO1 *fimV346*	PAO1 transposon mutant, Tn5 *lux* insertion at position 346 in *fimV*	Wehbi et al, 2011
PAO1 *fimV2091*	PAO1 transposon mutant, Tn5 *lux* insertion at position 2091 in *fimV*	Wehbi et al, 2011
PAO1 *fimV1194*	PAO1 with SmaI-flanked FRT insertion at position 1194 (SmaI) in *fimV*	Wehbi et al, 2011
PAO1 *pilG*	In-frame deletion of *pilG*	Bertrand et al, 2010
PAK *pilG*	In-frame deletion of *pilG*	Fulcher et al., 2010

PAO1 *pilH*	PAO1 with SmaI-flanked FRT insertion in *pilH*	Khalil, M.Sc Thesis
PAK *cyaAB*	Inframe deletions of both the *cyaA* and *cyaB* genes.	Fulcher et al., 2010
PAO1 *fimV346* + pFimV6His	*fimV346* mutant complemented with pUCP20Gm-*fimV*; full-length *fimV* gene in pUCP20Gm with C-terminal 6xHis-tag	Wehbi et al, 2011
PAO1 *fimV2091*+ pFimV6His	*fimV2091* mutant complemented with pUCP20Gm-*fimV;* full-length *fimV* gene in pUCP20Gm with C-terminal 6xHis-tag	Wehbi et al, 2011
PAO1 *fimV1194* + pFimV6His	*fimV1194* mutant complemented with pUCP20Gm-*fimV*; full-length *fimV* gene in pUCP20Gm with C-terminal 6xHis-tag	Wehbi et al, 2011
PAO1 *fimV346* + pFimV	*fimV346* mutant complemented with pUCP20Gm-*fimV*; full-length *fimV* gene in pUCP20Gm	This study
PAO1 *fimV2091*+	*fimV2091* mutant complemented	This study

pFimV	with pUCP20Gm-*fimV*; full-length *fimV* gene in pUCP20Gm	
PAO1 *fimV1194* + pFimV	*fimV1194* mutant complemented with pUCP20Gm-*fimV*; full-length *fimV* gene in pUCP20Gm	This study
PAO1 pilG + pPilG	*pilG* mutant complemented with pUCP20Gm-*pilG*; full-length *pilG* gene in pUCP20Gm	Khalil M.Sc Thesis
PAO1 *pilH* + pPilH	*pilH* mutant complemented with pUCP20Gm-*pilH*; full-length *pilH* in pUCP20Gm	Khalil M.Sc Theis
PAO1 + pMarkiN	The PAO1 strain carrying the YFP vector	This study
PAK + pMarkiN	The PAK strain carrying the YFP vector	This study
PAO1 + pMarkiC*:pilG*	The PAO1 strain complemented with the PilG-YFP C-terminal fusion in pMarkiC	This study

PAK + pMarkiC:*pilG*	The PAK strain complemented with the PilG-YFP C-terminal fusion in pMarkiC	This study
PAO1 *pilG* + pMarkiN	The PAO1 *pilG* strain carrying the YFP fluorescent vector	This study
PAK *pilG* +pMarkiN	The PAK *pilG* strain carrying the YFP fluorescent vector	This study
PAO1 *pilG* + pMarkiC:*pilG*	The PAO1 *pilG* strain complemented with the PilG-YFP C-terminal fusion in pMarkiC	This study
PAK *pilG* + pMarkiC:*pilG*	The PAK *pilG* strain complemented with the PilG-YFP C-terminal fusion in pMarkiC	This study
PAK *cyaAB* + pMarkiN	The PAK *cyaAB* strain carrying the YFP fluorescent vector	This study
PAK *cyaAB* + pMarkiC:*pilG*	The PAK *cyaAB* strain complemented with the PilG-YFP C-terminal fusion in pMarkiC	This study

PAO1 *fimV346* + pMarkiN	The PAO1 *fimV346* strain carrying the YFP fluorescent vector	This study
PAO1 *fimV346* + pMarkiC:*pilG*	The PAO1 *fimV346* strain complemented with the PilG-YFP C-terminal fusion in pMarkiC	This study
PAO1 fimV2091 + pMarkiN	The PAO1 *fimV2091* strain carrying the YFP fluorescent vector	This study
PAO1 *fimV2091* + pMarkiC:*pilG*	The PAO1 *fimV2091* strain complemented with the PilG-YFP C-terminal fusion in pMarkiC	This study
PAO1 *fimV1194* + pMarkiN	The PAO1 *fimV1194* strain carrying the YFP fluorescent vector	This study
PAO1 fimV1194 + pMarkiC:*pilG*	The PAO1 *fimV1194* strain complemented with the PilG-YFP	This study

	C-terminal fusion in pMarkiC	
PAO1 + pUCP20Gm	The PAO1 strain complemented with the pUCP20Gm as vector control	This study
Plasmids		
pET151	T7 inducible expression vector encoding a TEV cleavable N-terminal 6xHis-V5 epitope tag	Invitrogen
pET151:fimV67-387	Expression construct for the N-terminal segment (residues 23 to 129) of FimV	Wehbi et al, 2011
pET151:*fimV67-762*	Expression construct for the N-terminal segment (residues 23 to 254) of FimV	Wehbi et al, 2011
pET151:*fimV1462-2760*	Expression construct for the soluble cytoplasmic region of FimV	This Study

pET151:*fimV1462-1902*	Expression construct for the TPR1 motif	This Study
pET151:*fimV2584-2760*	Expression construct for the TPR2 motif	This Study
pET151:*pilG*	Expression construct for the chemotaxis protein PilG	Khalil et al, manuscript in preparation
pET151:*pilH*	Expression construct for the chemotaxis protein PilH	Khalil et al, manuscript in preparation
pET28a:*fimV66-1170*	Expression construct for the N-terminal segment (residues 23 to 390) of FimV	Wehbi et al, 2011
pUCP20Gm	Shuttle vector with SmaI-flanked Gm cassette inserted into ScaI site in bla	Chiang et al, 2003
pFimV6His	*fimV* complementation construct encoding full-length FimV; cloned in the ScaI and XbaI sites of the vector including C-terminal 6xHis-	Wehbi et al, 2011

	tag	
pFimV	*fimV* complementation construct encoding full-length FimV; cloned in the ScaI and XbaI sites of the vector	This study
pMarkiN	pUCP20Gm vector containing gene encoding YFP; for N-terminal fusions	Chiang et al, 2005
pMarkiC	pUCP20Gm vector containing gene encoding YFP; for C-terminal fusions	Chiang et al, 2005
pMarkiC:*pilG*	*pilG* gene cloned into the pMarkiC vector at the SmaI site	Khalil M.Sc Thesis

Table 2. List of oligonucleotides used.

Primer	**Oligonucleotide Sequence**
fimV67	5'-CAC CCA TGG ATT GGG ACT GGG GGA AAT CA-3'
fimV387	5'-TCA CAG CAG GAC GGT GTA CTC GCG CAG CA-3'
fimV762	5'-TC CCA GCT CTG GTT CTG CGC CTG CAC CT-3'
fimV1462	5'-CAC CAA TGC GCA GAA AGA GGA A-3'
fimV1902	5'-TCA GGC CAG GGC AAC CGC-3'
fimV2584	5'-CAC CGA TGA CTT CGA CTT CCT CTC CGG TGC-3'
fimV2760	5'-TCA GGC CAG GCG CTC CAG CAA CTC-3'
fimV His Stop Forward	5'-AGT TGC TGG AGC GCC TGG CCT GAC ACC ACC ACC ACC-3'
fimV His Stop Reverse	5'-TGG TGG TGG TGG TGT CAG GCC AGG CGC TCC AGC AC-3'

Table 3. List of antisera used and dilution factors

Antisera	Dilution
A-PilM	1:1000
A-PilN	1:1000
A-PilO	1:3000
A-PilP	1:2000
A-PilG	1:2000
A-PilH	1:2000
A-PilA	1:3000
A-6His (Santa Cruz)	1:3000

A-Rabbit (secondary)	1:3000
A-mouse (secondary)	1:3000

Table 4. Summary of PilG Localization Data

Strain expressing PilG-YFP	PilG Localization
PAO1	POLAR
PAK	POLAR
*E. coli*DH5α	DIFFUSE
PAO1 *pilG*	POLAR
PAK *pilG*	POLAR
PAK *cyaAB*	POLAR
PAO1 *pilH*	POLAR

fimV346	DIFFUSE
fimV2091	DIFFUSE
fimV1194	DIFFUSE

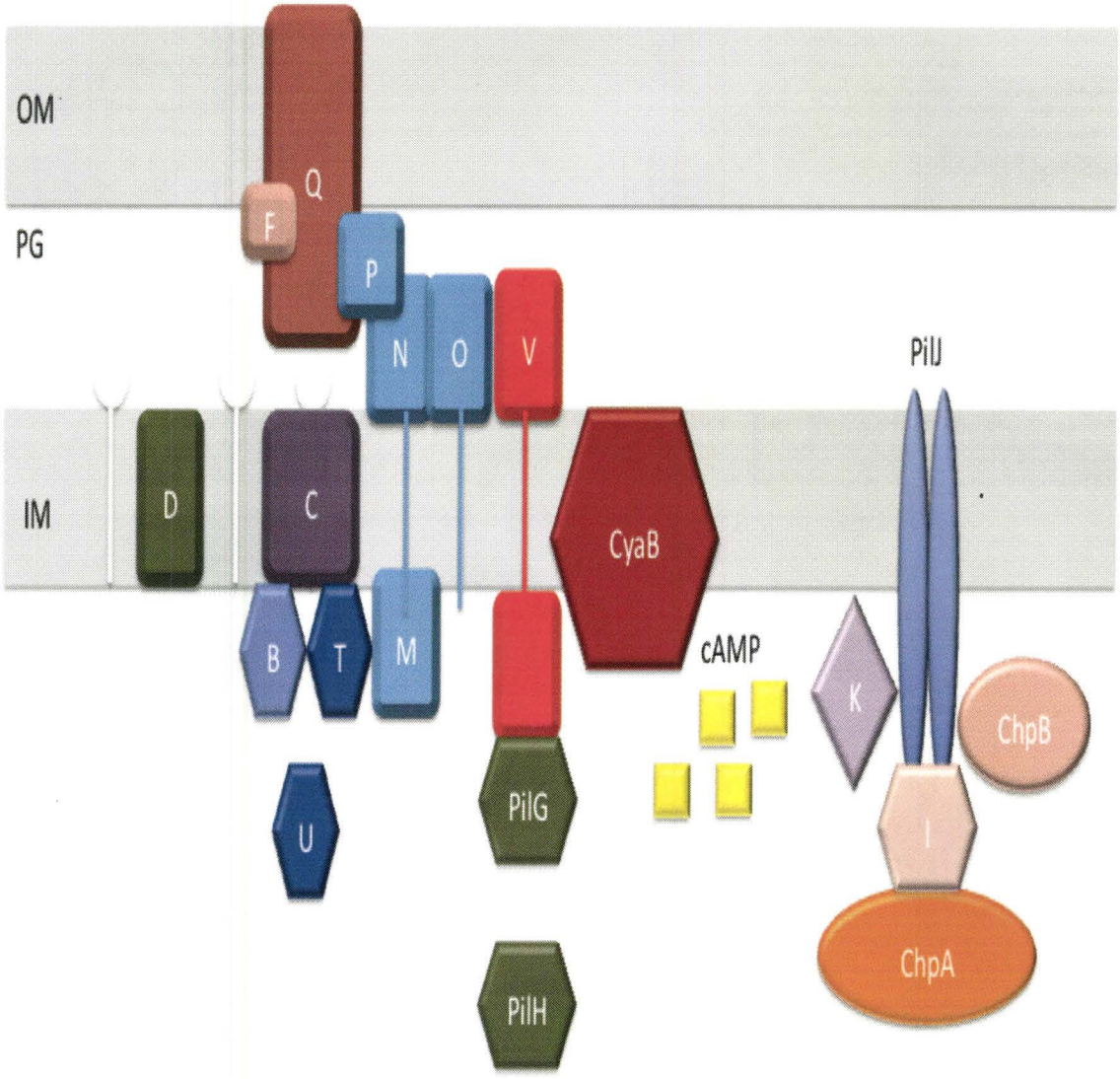

Figure 1. A schematic representaion of the current model exhibiting some of the proteins involved in the Type 4 Pilus system in *Pseudomonas aeruginosa.*

Figure 1. A schematic representaion of the current model exhibiting some of the proteins involved in the Type 4 Pilus system in *Pseudomonas aeruginosa.*

The major pilin subunit is processed by the pre-pilin peptidase PilD. PilC is an inner membrane platform protein and the ATPases, PilB and PilT associate/dissociate the major pilin to form the pilus fibre. The PilQ secretin pore, stabilized by PilF, facilitates the passage of the pilus through the outer membrane. Inner membrane complex PilM/N/O/P directs the pilus fibre to PilQ. FimV, bound to peptidoglycan, promotes the assembly of the secretin and is associated with the inner membrane complex. PilJ senses chemical stimuli and undergoes a confimational change that leads to its methylation by a methyltransferase. This methylation event causes the autophosphorylation of ChpA, which then goes on to phosphorylate PilG. FimV and PilG form a subcomplex that increases CyaB activity, leading to increased levels of intracellular cAMP.

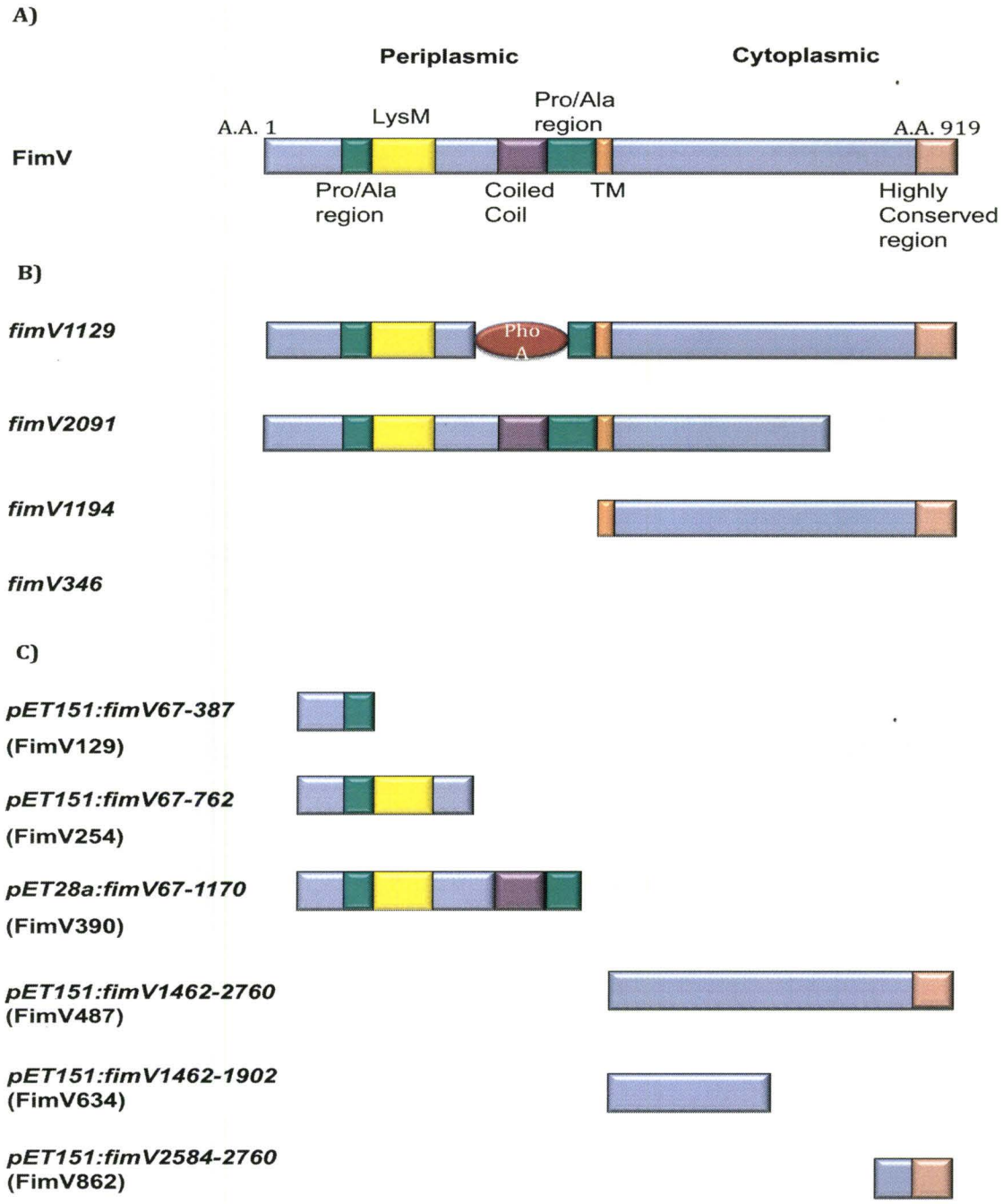

Figure 2. A schematic representation of the FimV domains and gene expression products.

Figure 2. A schematic representation of the FimV domains and gene expression products.

A) The full length model of FimV from PAO1 is depicted indicating the structural and functional proline/alanine rich regions (P/A; green), LysM domain (yellow), coiled coil (CC; purple), transmembrane domain (TM; orange) and a highly conserved C-terminal region (pink). B) Fragments of FimV expressed from mutant strains. Protein fragments were detected by western blot analysis using antibodies raised to the cytoplasmic or periplasmic region. C) Expression products from the IPTG inducible T7 over expression vector, used for expression in *E. coli* BL21 (DE3).

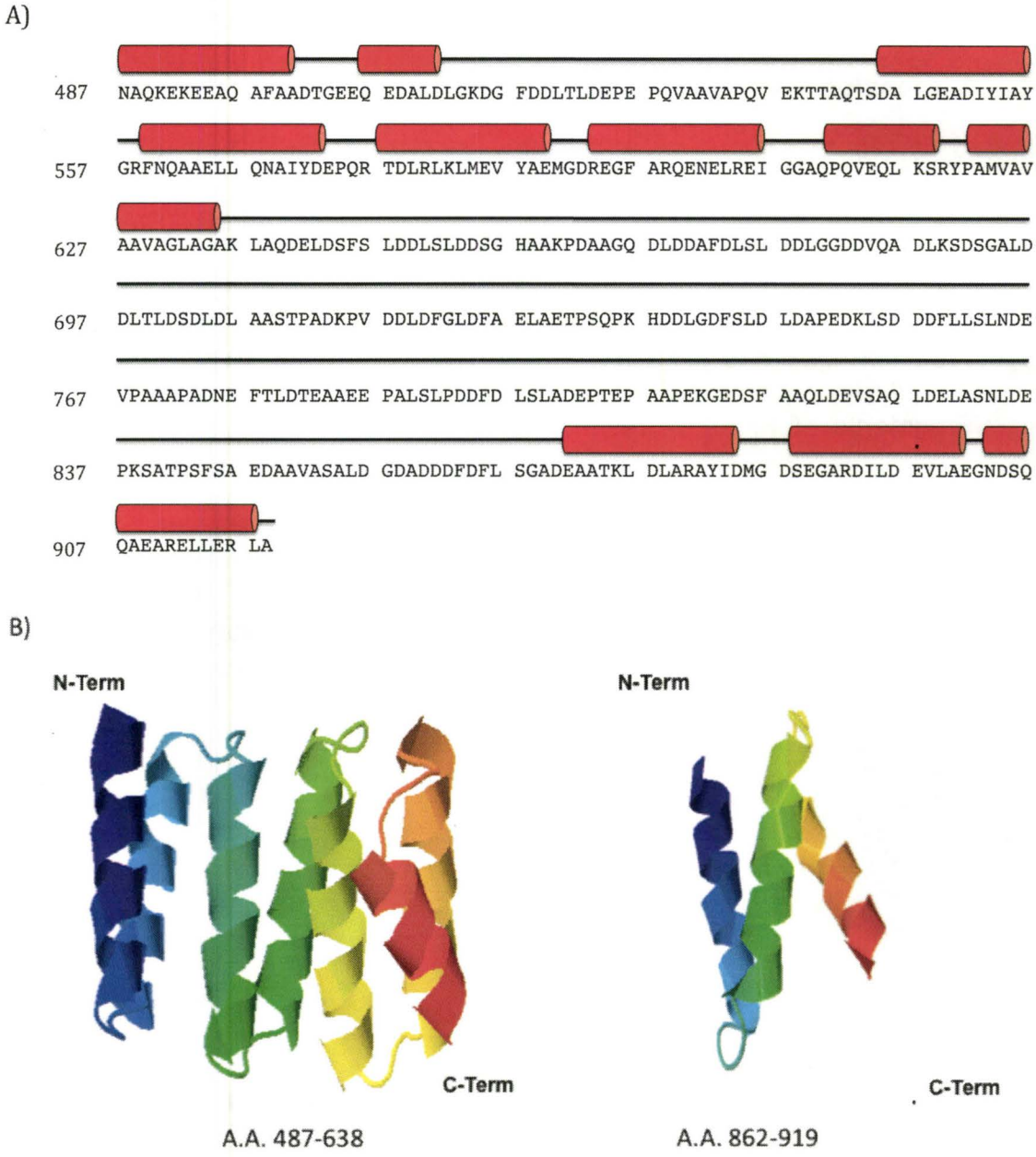

Figure 3. Secondary structure and protein fold prediction of the cytoplasmic region of FimV.

Figure 3. Secondary structure and protein fold prediction of the cytoplasmic region of FimV.

A) The primary sequence of FimV from residues 487-919 were input into the Psipred, PHYRE and Jpred online secondary structure prediction software programs. The programs were set to exclude any α-helices that were predicted to be transmembrane segments. An average of the predicted secondary structure is depicted. The red cylinders are regions predicted to be α-helical, where as the black lines are predicted to be unstructured. B) The primary sequence of FimV was compared against known protein folds using the online software program PHYRE. Many TPR-like motifs were recognized by this search with high estimated precision (>99%) low E-values (9.9e^-12 to 5.8e^-11), including the two structures included in this figure. From residues 509 – 621, PHYRE predicts a TPR-like motif similar to that of a synthetic consensus TPR protein (Kajander et al., 2007). A TPR-like motif was predicted for the highly conserved C-terminal region mapped onto a portion of cyclophilin 40.

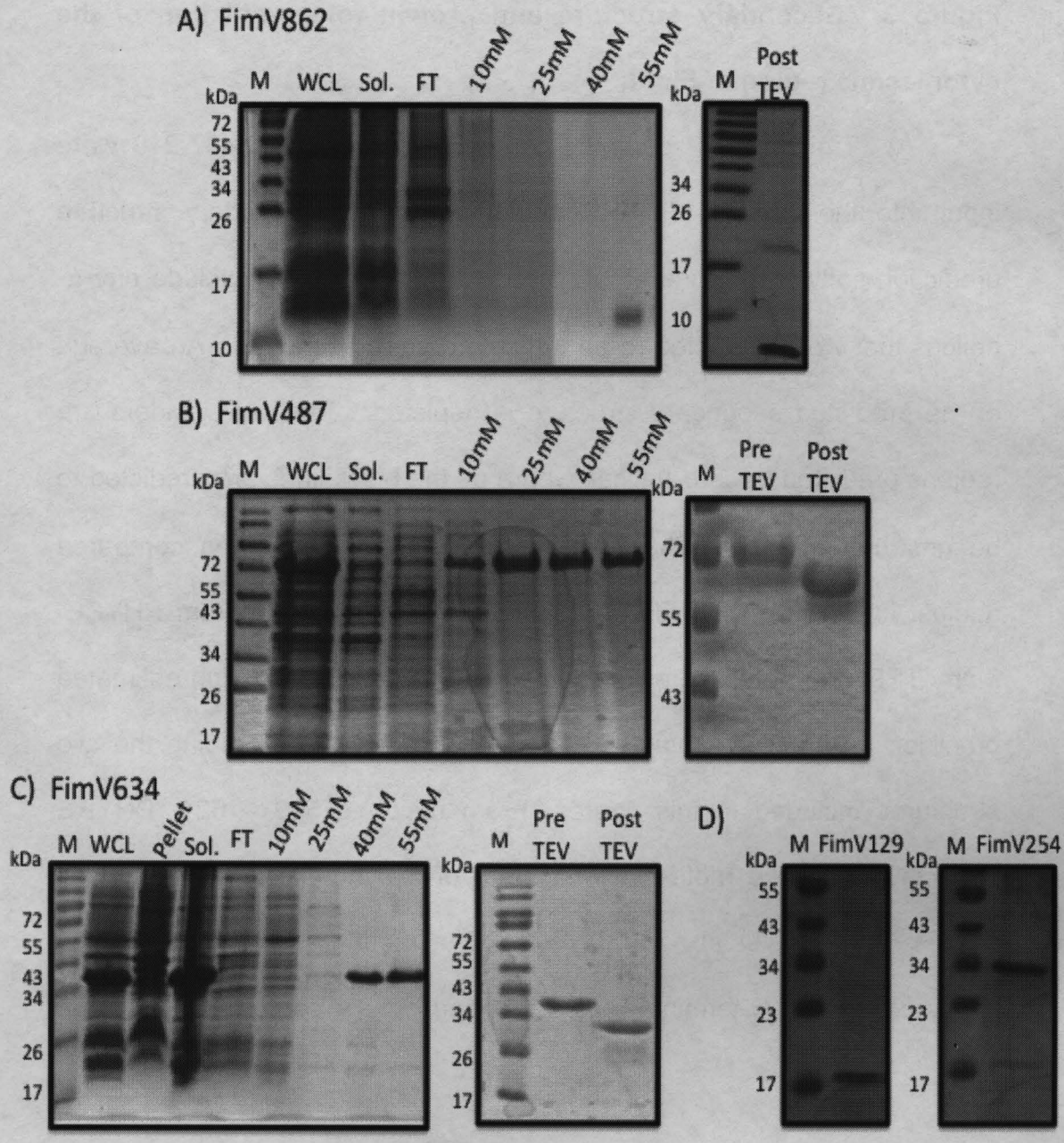

Figure 4. The purification of FimV fragments using nickel chromatography and TEV proteolysis of purified proteins.

Figure 4. The purification of FimV fragments using nickel chromatography and TEV proteolysis of purified proteins.

Purification of His-tagged FimV fragments. Clarified lysate containing his-tagged FimV fragments were applied to a 5 mL Ni+ column. The column was subsequently washed with 20 mL wash steps of buffer containing increasing concentrations of imidazole (fractions collected at every wash step). Fractions were prepped with SDS loading buffer and visualized by SDS-PAGE gel. Fractions containing purified FimV fragments were then dialyzed overnight into a buffer containing 20 mM Tris pH8 and 100 mM KCl. The purified protein was then incubated with TEV protease for 2.5 hrs at room temperature. The reaction was quenched with the addition of 100 mM benzamidine. The reaction mixture was then applied to a 5 mL Ni+ column and the flow through was collected and analyzed by SDS PAGE. A) FimV862-919 eluted off the column in the 300 mM imidazole fraction, as confirmed by a western blot probing for cytoplasmic FimV. The α-CytoFimV antibody was raised against a purified C-terminal fragment of FimV containing a non-cleavable N-terminal His-tag. After TEV cleavage and concentration, a contaminant at 20 kDa was still present. B) FimV487 started to elute off the column at 25 mM imidizole but was most pure at 55 mM. C) FimV634 started to elute of the column at the 40 mM wash and was most pure at 55 mM. D) FimV129

and FimV254 both eluted off the column at the 300 mM wash step, where it was most pure.

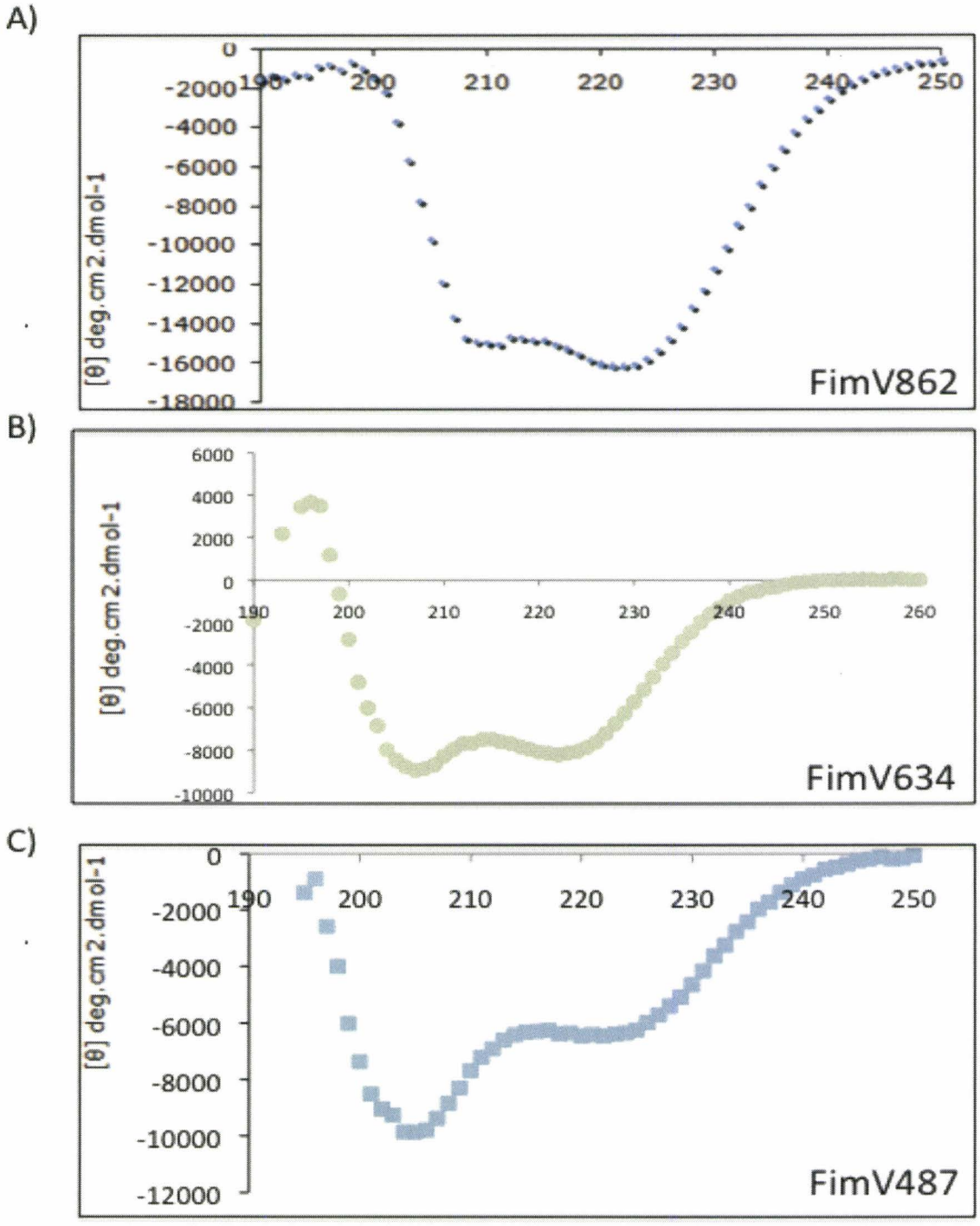

Figure 5. Circular dichroisim of the cytoplasmic domain shows α-helical content.

Figure 5. Circular dichroism of the cytoplasmic domain shows α-helical content.

Circular dichroism spectroscopy of purified FimV862, FimV634 and FimV487. Protein samples were prepared in PBS at a concentration of 0.5 mg/mL. Buffer spectra was taken and subtracted from the sample spectra to account for background absorbance. The absorbance spectra were converted to molar ellipticity with respect to the number of amino acids. Local minima can be seen at around 208 nm and 222 nm, characteristic of α-helical folds. A) The molar ellipticity of FimV862 displays the most characteristic of an α-helical protein with minima at approximately -16000 θ. B) FimV632 had calculated values for molar ellipticity of -8900 θ and -8100 θ at 208 and 222 nm respectively. C) FimV487 also had an α-helical CD signature with its higher wavelength local minima at 222 nm calculated at -6500 θ, however, with its local minima blue-shifted to 206 nm with a value of -10000 θ.

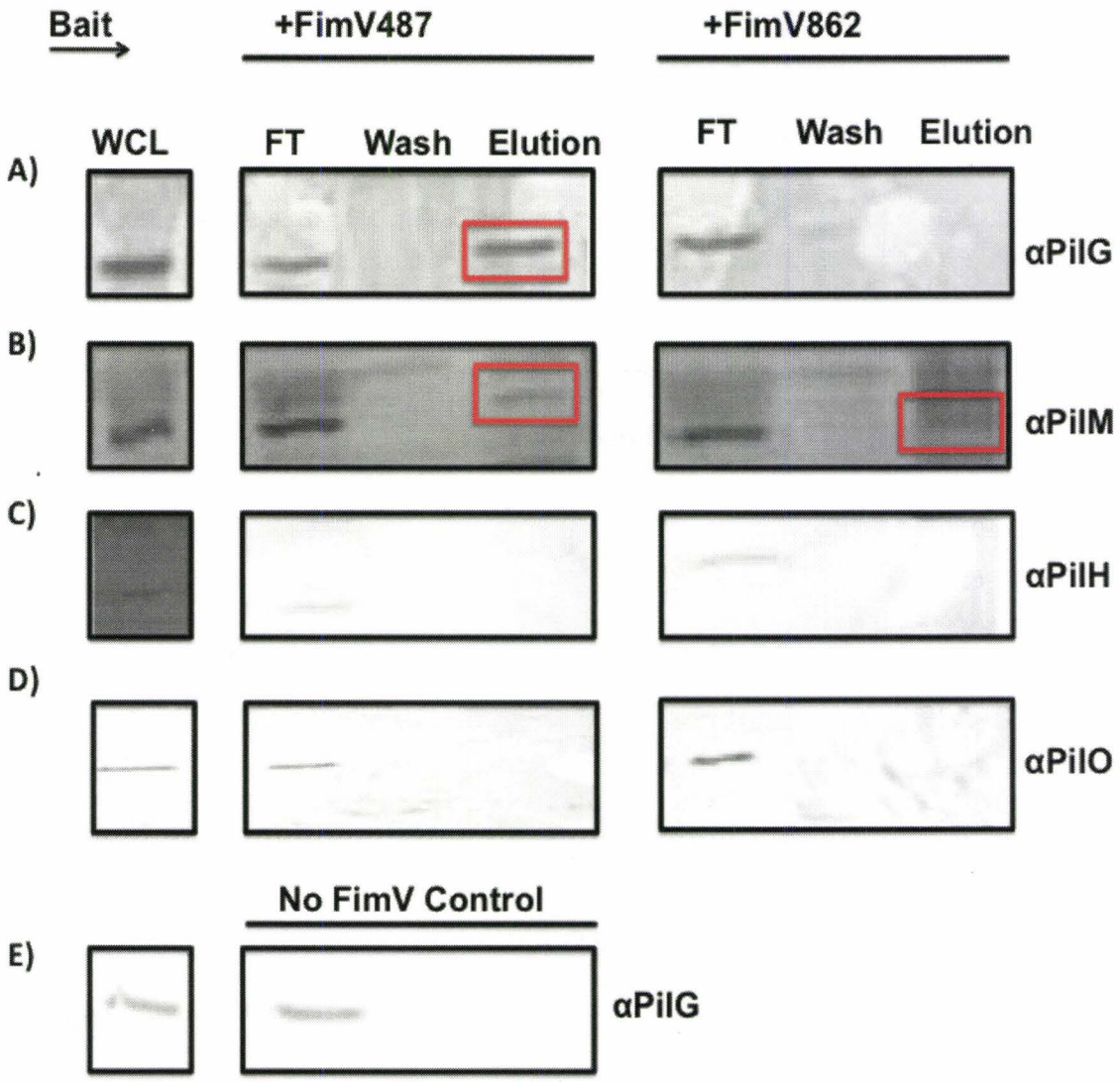

Figure 6. FimV co-purifies with chemotaxis protein PilG and inner membrane complex protein PilM.

Figure 6. FimV co-purifies with chemotaxis protein PilG and inner membrane complex protein PilM.

Western blots of collected fractions were probed with indicated antibody. FimV487 and FimV862 were over-expressed in *E. coli* BL21 and purified using Ni chromatography and size exclusion chromatography. FimV487 and FimV862 were then subsequently added to the whole cell lysates of PAO1. The whole cell lysate mixture was then added to a 5 mL Ni column, where it was washed with 25 mL of wash buffer containing 200 mM NaCl and 10 mM imidazole. Proteins were eluted with elution buffer containing 300 mM imidazole. A) A band in the elution fraction indicates the presence of PilG when bound to FimV487, however, PilG is not detected when FimV862 is immobilized on the Nickel resin. B) A band in the elution fractions indicates the presence of PilM when bound to both FimV487 and FimV862. C)-D) Negative controls, as PilH and PilO do not co-purify with either FimV fragment. E) Another negative control, showing the inability of PilG to bind to the nickel resin with no His-tagged protein present.

A)

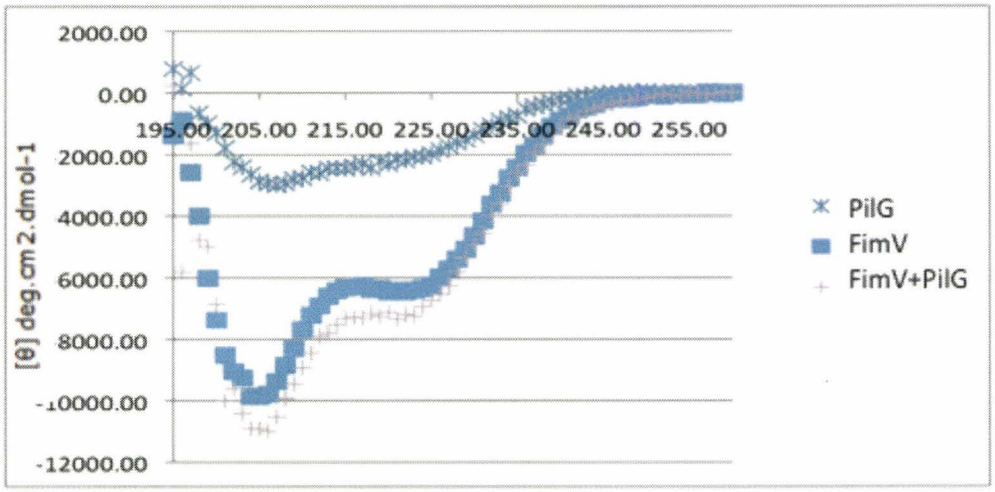

B)

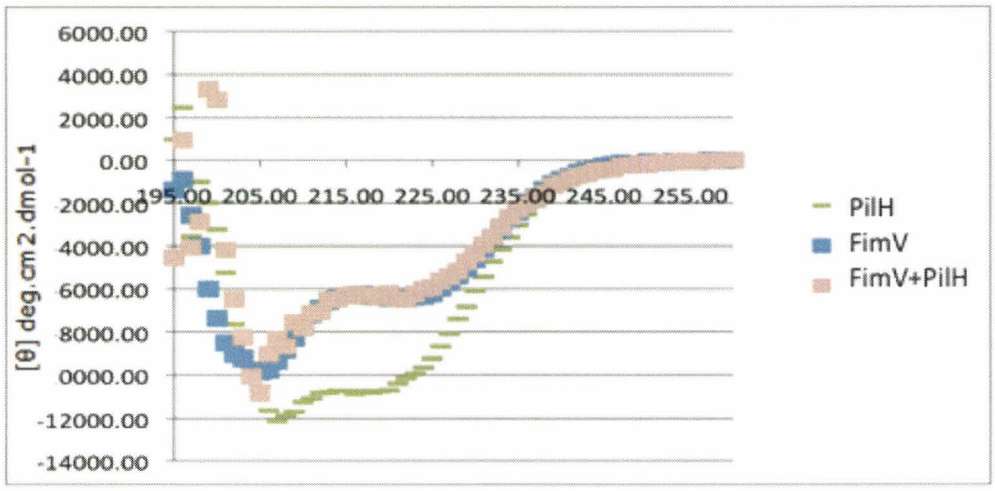

Figure 7. FimV moderately gains α-helical secondary structure upon incubation with PilG.

Figure 7. FimV moderately gains α-helical secondary structure upon incubation with PilG.

Incubation with PilG induces minimal change in the secondary structure of FimV. The circular dichroism spectra of FimV incubated with and with out PilG or PilH. The Y-axis is in units of molar ellipticity and the X-axis is the wavelength in nm. Shown also are controls of PilG alone (PilG 1:3) and PilH alone (PilH 1:3). A) When FimV is incubated with PilG in a 1:3 molar ratio (1:3) an appreciable shift is observed compared to FimV alone (FimV alone). B) As a negative control, the experiment was repeated using PilH as the potential interaction partner. A 10% increase in magnitude of molar ellipticiy is observed only when FimV is incubated with PilG.

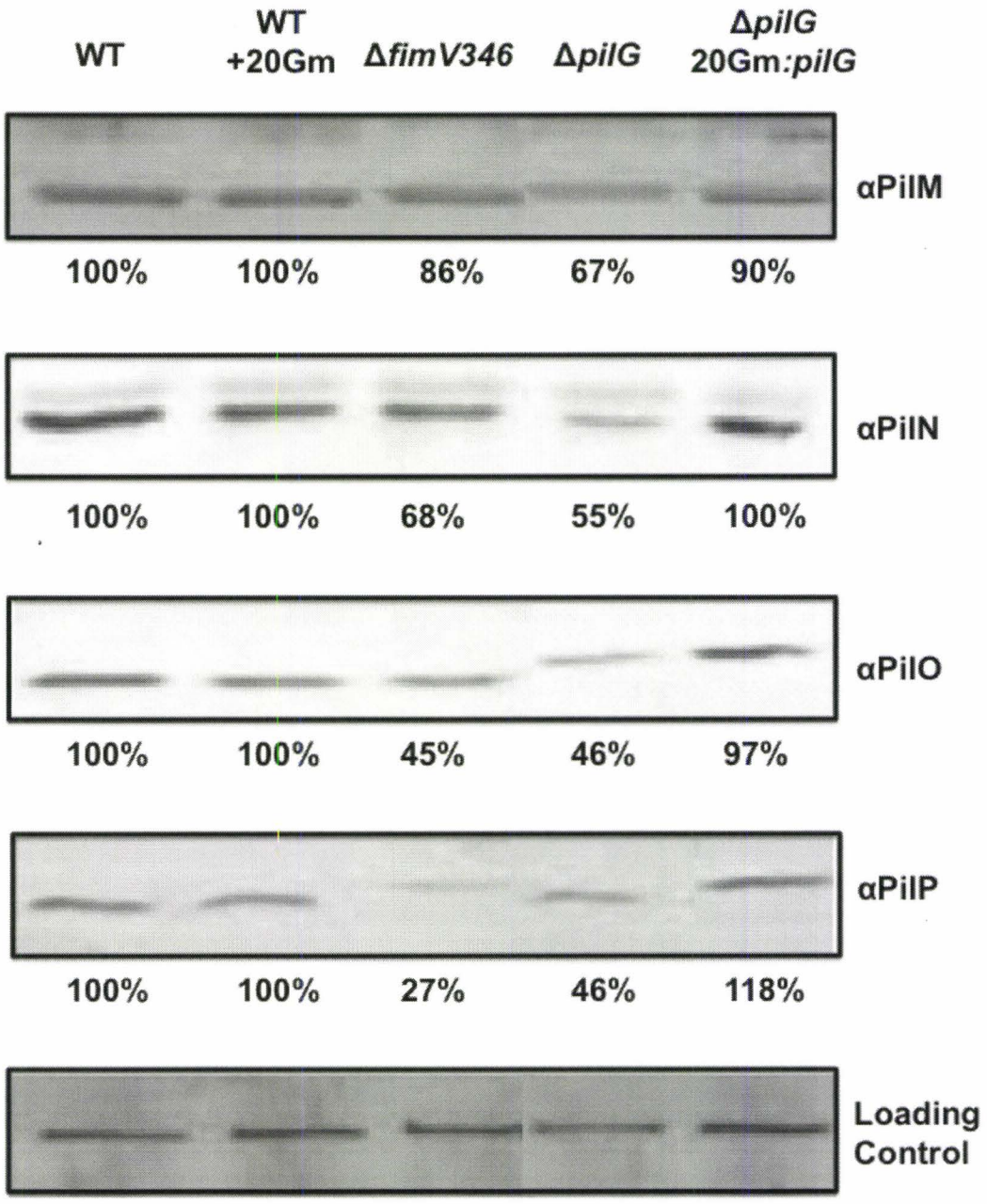

Figure 8. *fimV and pilG* mutants have lower expression of the inner membrane complex proteins PilMNOP.

Figure 8. *fimV and pilG* mutants have lower expression of the inner membrane complex proteins PilMNOP.

Specified strains were subcultured from overnight cultures to fresh LB media and grown to mid-log phase of growth (O.D. 0.6). Cells were lysed in SDS sample buffer and boiled. Samples were probed with antibodies specific to PilM, PilN, PilO, or PilP. Band intensities were measured against internal loading controls (non-specific bands) using ImageJ software and then reported as Percent WT control. A) A 23% reduction of PilM levels were observed in the *pilG* mutant. B) The *pilG* mutant had a 45% reduction of PilN levels. C) Only 46% of PilO was observed in the *pilG* mutant. D) The western blot of PilP indicated only 46% of PilP present in the whole cell lysate of the *pilG* mutant.

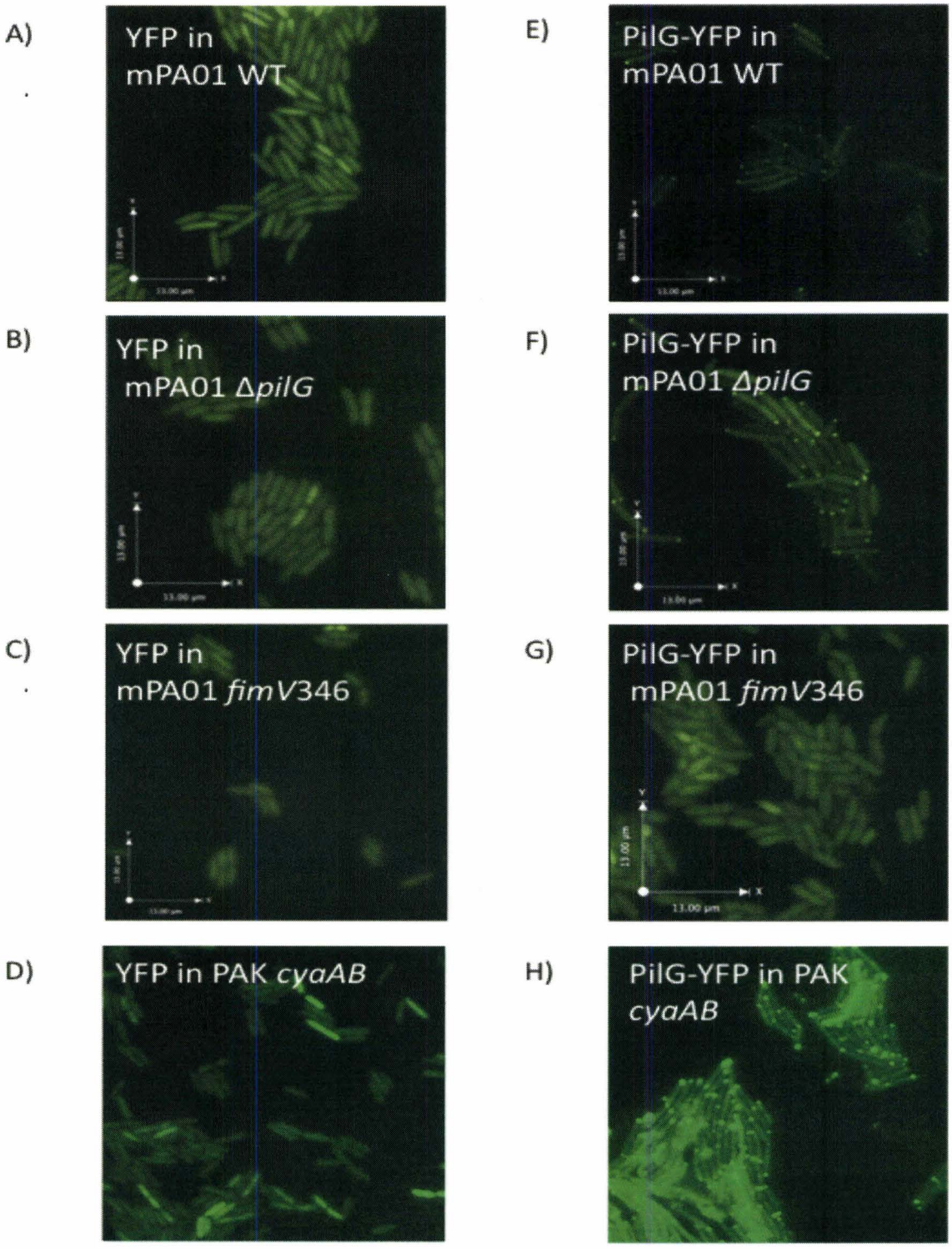

Figure 9. PilG localization is affected by the absence of FimV.

Figure 9. PilG localization is affected by the absence of FimV.

PilG-YFP C-terminal fusions were generated in the pUCp20Gm vector and electroporated into the specified strains. Cells were streaked and grown on LB-Agar plates with appropriate antibiotic. Cells from the periphery of the growth zones were then transported to the coverslips and viewed on a wide-field deconvolution microscope. PAO1 strains lacking FimV displayed PilG mis-localization.

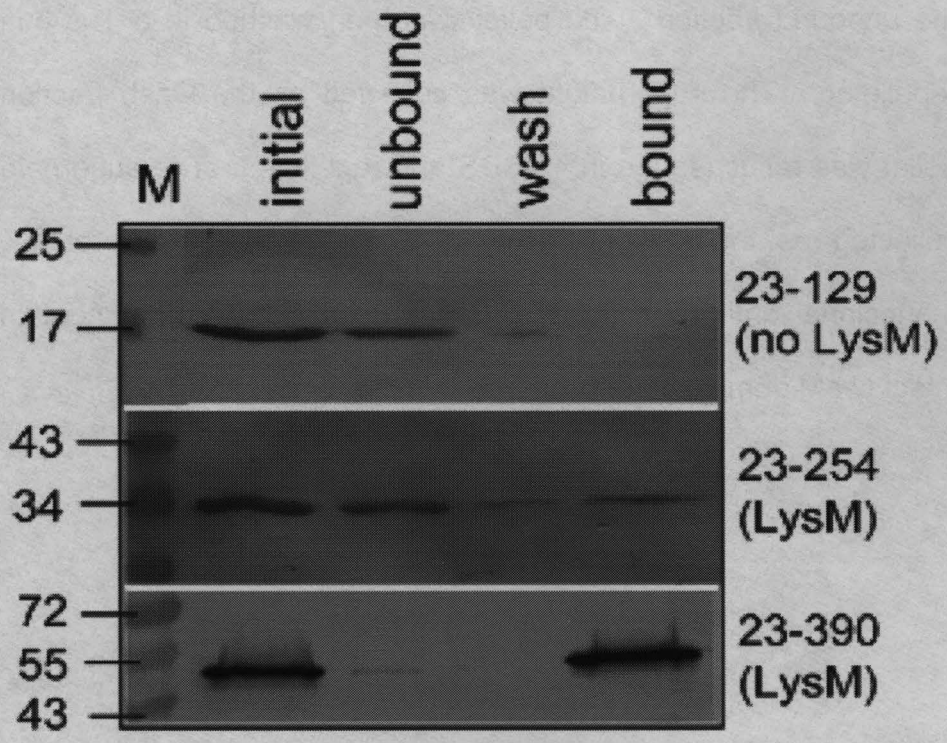

Figure 10. FimV's LysM domain is required for PG binding.

Figure 10. FimV's LysM domain is required for PG binding.

Western blot analysis of collected fractions from the PG pulldown assay. Truncated versions of FimV were incubated with PG and centrifuged to pellet PG. The supernatant was removed and collected as the unbound fraction. The pellet was then washed in a Tris buffer and repelleted. The supernatant was collected as the wash fraction. The pellet was resuspended in 4%SDS and repelleted. The supernatant was collected as the elution fraction. Each fraction was probed with a monoclonal anti-His antibody. Only truncations of FimV containing an intact LysM domain were observed in the bound fraction.

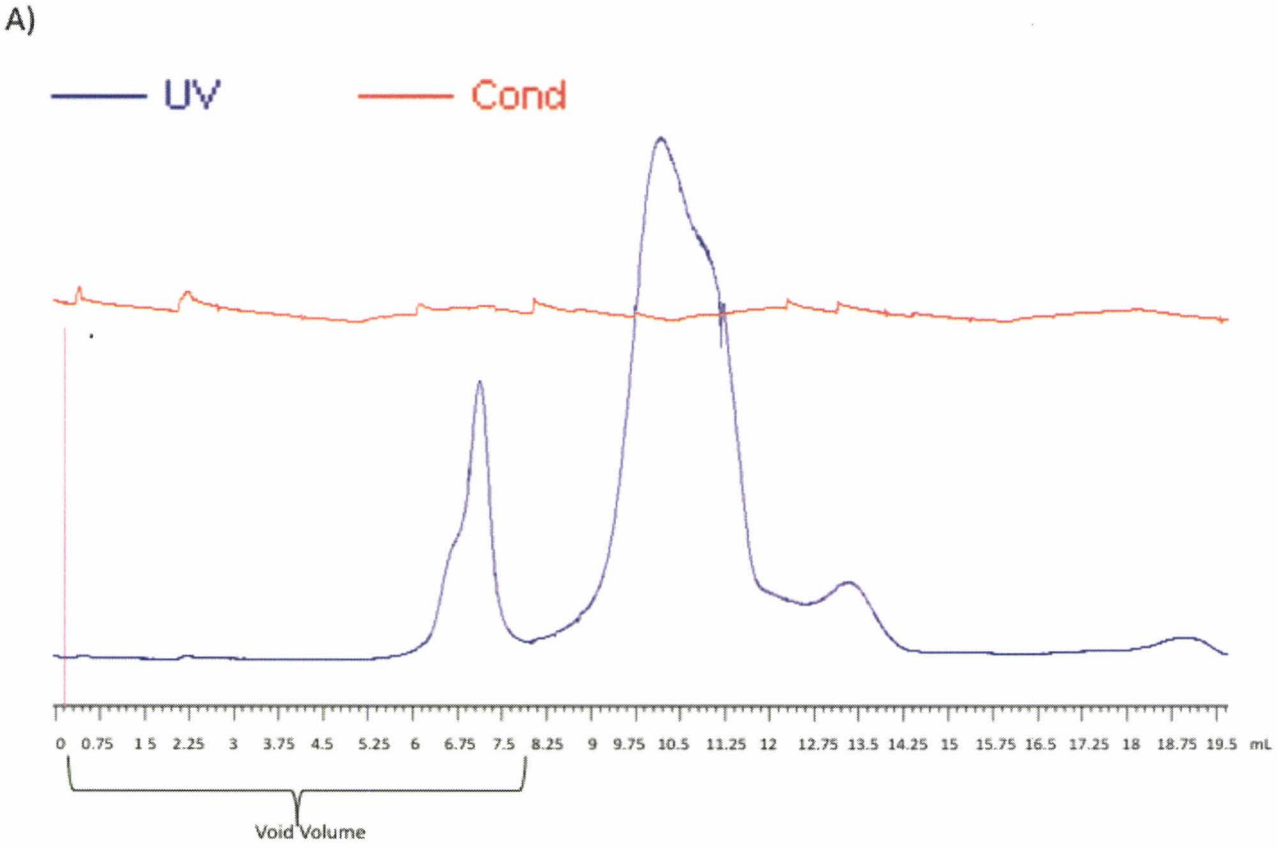

Figure 11. Gel filtration purification of cytoplasmic FimV.

Figure 11. Gel filtration purification of cytoplasmic FimV.

FimV487 was further purified by size exclusion chromatography. FimV487 was concentrated to 15 mg/mL and injected onto a pre-equilibrated superdex200 column. Eluted materials were monitored by UV absorption. A) A chromatogram of the protein elution profile from gel filtration. The first peak begins at 6 mL and is void volume. The next peak and shoulder begin at 9 mL and contains the higher molecular weight FimV487. The next minor peaks at 13 and 19 mL are believed to be contaminating proteins or FimV487 degradation products. B) SDS-PAGE analysis of the gel filtration procedure. In the pre-injected sample, multiple bands are visualized by the Coomassie stain where as in the post gel filtrated sample, fewer bands are visible.

A)

B)

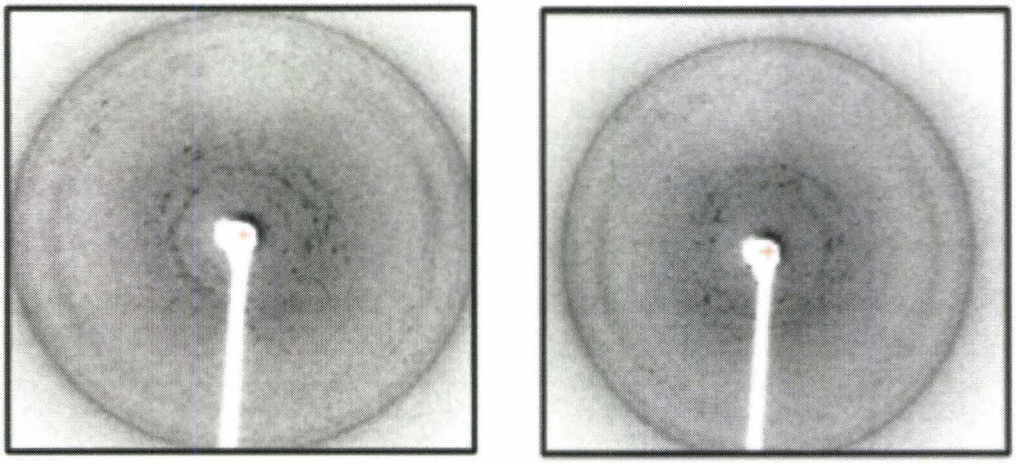

Figure 12. Protein crystals and diffraction patterns of FimV862.

Figure 12. Protein crystals and diffraction patterns of FimV862.

A) Light microscope image of the protein crystals set in a hanging drop. The protein crystals vary in size and shape. Crystals were grown over a week at 18°C at a protein concentration of 4 mg/mL. B) Diffraction patterns of FimV862 crystals shot with X-rays with a 10 minute exposure. Protein crystals were flash frozen directly in liquid nitrogen stream with no additional cryo-protectant prior to X-ray diffraction collection. The top and bottom diffraction patterns are taken from the same crystal with an orientation difference of 90°.

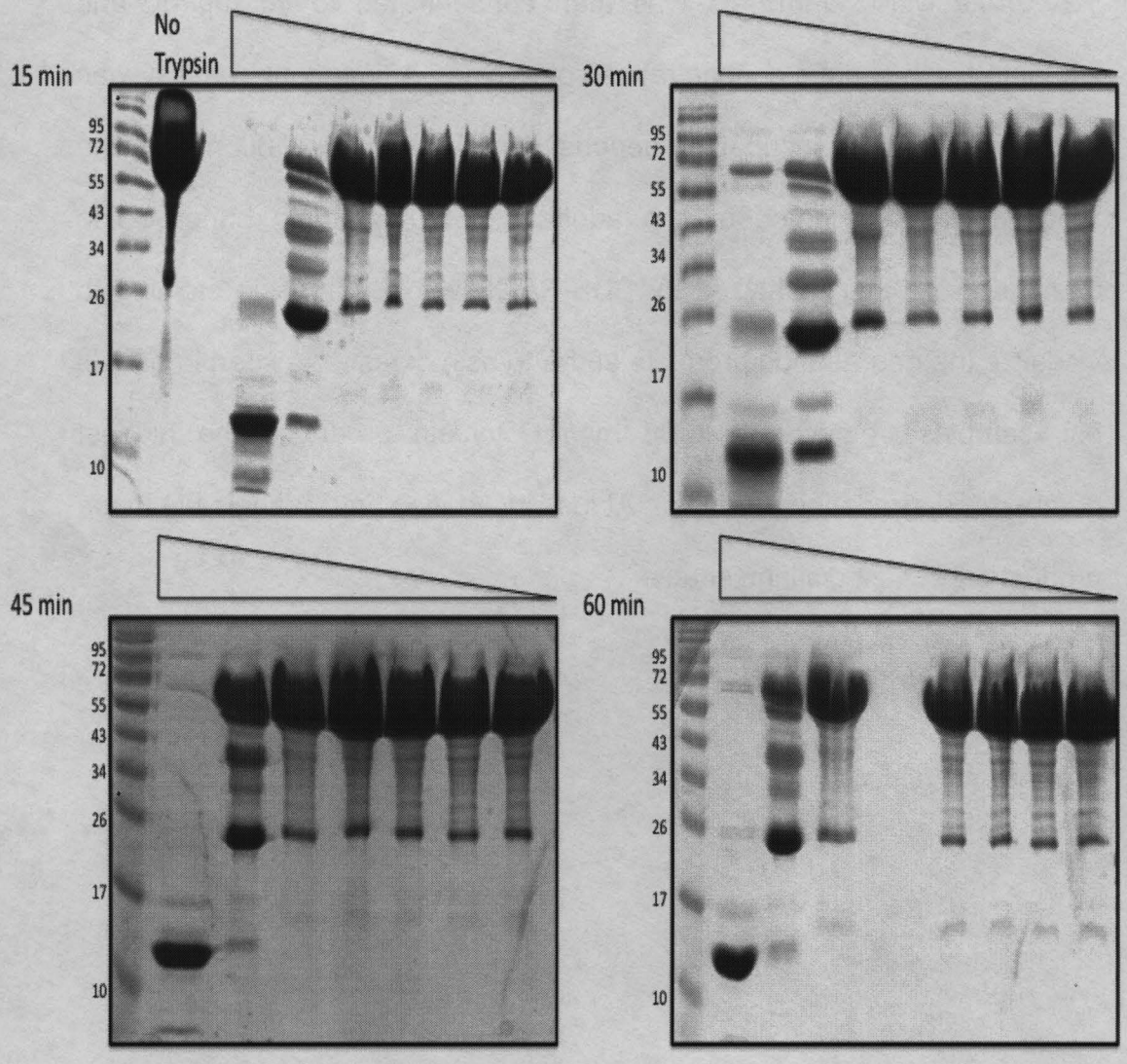

Figure 13. Partial proteolysis of FimV487 reveals stable structural cores.

Figure 13. Partial proteolysis of FimV487 reveals stable structural cores.

FimV487 was previously purified using nickel chromatography and TEV proteolysis. FimV487 was then concentrated to 10 mg/mL and incubated with various concentrations of trypsin. A time course assay was also performed as incubation periods varied from 15 – 60 min. The reaction was terminated by the addition of SDS-Sample buffer. The samples were then analyzed by SDS-PAGE with Coomassie staining to visualize the degradation products of the trypsin digest. As seen in panels i-iv, samples treated with 0.05 mg/mL trypsin produced the highest number of degradation products. At less incubation time (panels i-ii) these products are most distinguishable.

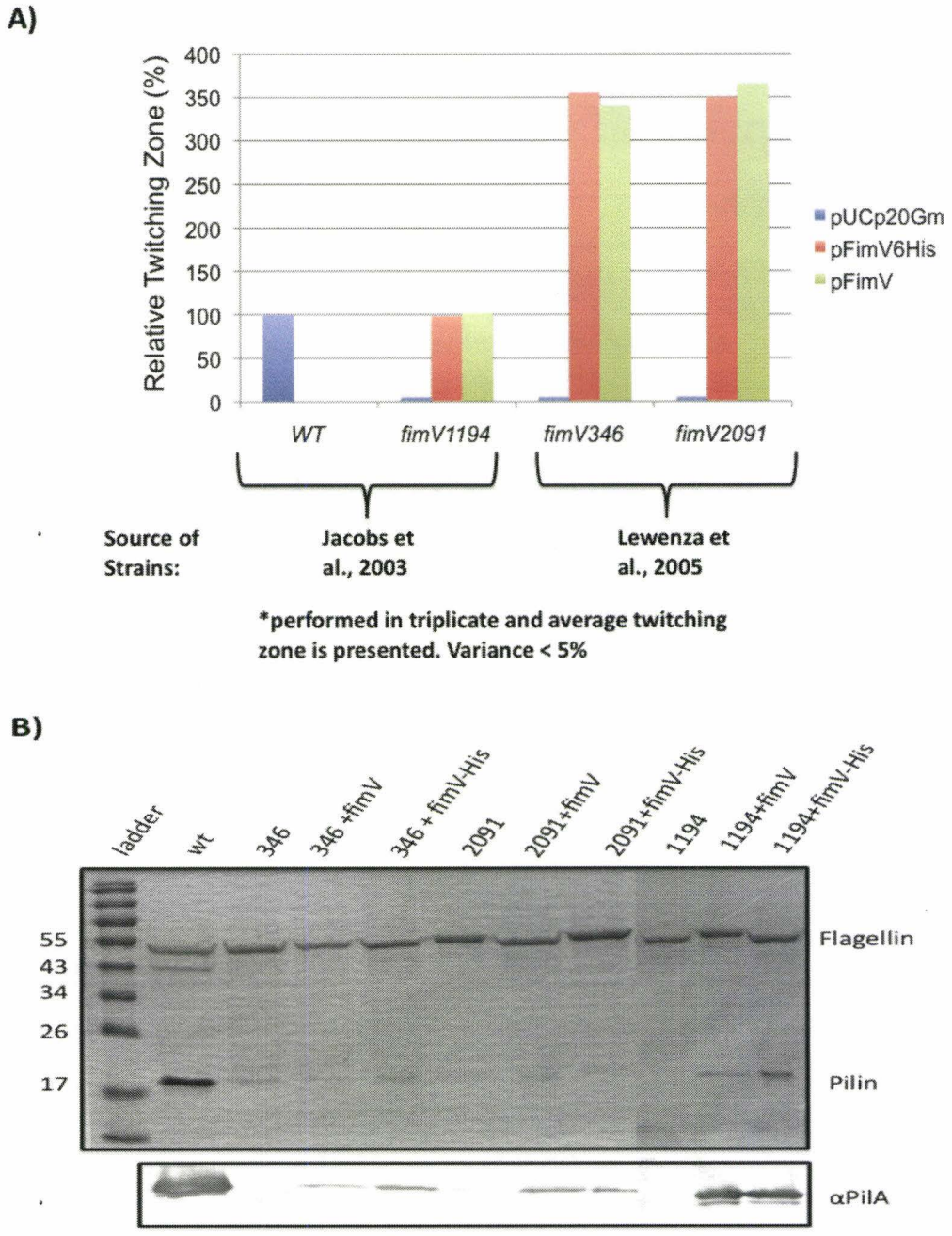

Figure 14. The differences in twitching zones and recoverable surface pili in the *fimV mutants* are due to the differences in the background PAO1 strains.

Figure 14. The differences in twitching zones and recoverable surface pili in the *fimV mutants* are due to the differences in the background PAO1 strains.

A) A graphical representation of the relative size of twitching zone compared to WT PAO1. There was no significant difference between complementation with or without the His-tagged complementation construct within each mutant, however significant differences are observed between complemented mutants. B) Sheared surface protein preparation of the complemented and uncomplemented *fimV* mutants. None of the complemented mutants restored wild-type levels of surface pili, however complemented *fimV1194* had the highest levels of recoverable surface pili.

REFERENCES

Ahn, K.S., Ha, U, Jia, J., Wu, D., and Jin, S. (2004). *The truA gene of Pseudomonas aeruginosa is required for the expression of the type III secretory genes. Microbiol.* **150:**539-547.

Alm, R.A., Hallinan, J.P., Watson, A.A., and Mattick, J.S. (1996). *Fimbrial biogenesis genes of Pseudomonas aeruginosa: pilW and pilX increase the similarity of type 4 fimbriae to the GSP protein-secretion systems and pilY1 encodes a gonococcal PilC homologue. Mol. Microbiol.* **22:**161-173.

Asherie, N. (2004). *Protein crystallization and Phase diagrams. Methods* 34,3:266-272.

Ast, V.M., Schoenhofen, I.C., Langen, G.R., Stratilo, C.W., Chamberlain, M.D., Howard, S.P. (2002). *Expression of the ExeAB complex of Aeromonas hydrophila is required for the localization and assembly of the ExeD secretion port multimer. Mol. Microbiol.* **44:**217 – 231.

Ayers, M., Sampaleanu, L.M., Tammam, S., Koo, J., Harvey, H., Howell, P.L., and Burrows, L.L. (2009). *PilM/N/O/P Proteins Form an Inner Membrane Complex That Affects the Stability of the Pseudomonas aeruginosa Type IV Pilus Secretin. J. Mol. Biol.* **394**:128 – 142.

Biais, N., Ladoux, B., Higashi, D., So, M., Sheetz, M. (2008). *Cooperative Retraction of Bundled Type IV Pili Enables Nanonewton Force Generation. PLoS Biol* 6(4): e87. doi:10.1371/journal.pbio.0060087

Bitter, W., Koster, M., Latijnhouwers, M., Cock, H., Tommassen, J. (1998). *Formation of oligomeric rings by XcpQ and PilQ, which are involved in protein transport across the outer membrane of Pseudomonas aeruginosa. Mol. Microbiol.* **27**:209 – 219.

Bodey, G.P., Bolivar, R., Fainstein, V., and Jadeja. (1983). *Infections caused by Pseudomonas aeruginosa.* Rev. Infect. Dis. **5**:279-313.

Buist, G., Steen, A., Kok, J., and Kuipers O.P. (2008). *LysM, a widely distributed protein motif for binding to (peptido)glycans. Mol. Micro.***68:**838-847.

Burrows, L.L. (2005). *Weapons of mass retraction. Mol. Micro.* **57:**878-888.

Carbonnelle, E., Helaine, S., Nassif, X. and Pelicic, V. (2006). *A systematic genetic analysis in Neisseria meningitidis defines the Pil proteins required for assembly, functionality, stabilization and export oftype IV pili. Mol. Micro.* **61**:1510 – 1522.

Castric, P. (1995). *pilO, a gene required for glycosylation of Pseudomonas aeruginosa 1244 pilin. Microbiol.* **141:**1247-1254.

Chiang, P. and Burrows, L. L. (2003). *Biofilm formation by hyperpiliated mutants of Pseudomonas aeruginosa. J. Bac.* **185**:2374–2378.

Chiang, P., Habash, and Burrows, L.L. (2005). *Disparate Subcellular Localization Patterns of Pseudomonas aeruginosa Type IV Pilus ATPases Involved in Twitching Motility. J. Bacteriol.* **187**: 829–839.

Chung, C.T., Niemela, S.L., and Miller, R.H. (1989). *One-step preparation of competent Escherichia coli: transformation and storage of bacterial cells in the same solution. PNAS.* **86**:2172-2175

Clarke, A.J. (1993). *Compositional analysis of peptidoglycan by high performance anion-exchange chromatography. Anal. Biochem.* **212**:344–350.

Cleveland, D.W., Fischer, S.G., Kirschner, M.W. and U.K. Laemmli (1977). *Peptide mapping by limited proteolysis in sodium dodecyl sulfate and analysis by gel electrophoresis. J. Biol. Chem.* **252:**1102-1106.

Costerton, J.W., Stewart, P.S., and Greenberb, E.P. (1999). *Bacterial biofilms: a common cause of persistent infection. Science* **284**:1318-1322.

Darzins, A. (1993) *The pilG gene product, required for Pseudomonas aeruginosa pilus production and twitching motility, is homologous to the enteric, single-domain response regulator CheY. J. Bac.* **175:**5934-5944.

Darzins, A. (1994) *Characterization of a Pseudomonas aeruginosa gene cluster involved in pilus biogenesis and twitching motility: sequence similarity to the chemotaxis proteins of enterics and gliding bacterium Myxococcus xanthus. Mo. Micro.* **11:**137-153.

Darzins, A. (1995). *The Pseudomonas aeruginosa pilK gene encodes a chemotactic methytransferase (CheR) homolog that is translationally regulated. Mol. Micro.***15**:703-717.

Dong, A. et al (2007) *In situ proteolysis for protein crystallization and structure determination. Nat. Methods.* **4**: 1019 – 1021.

Dower, W.J., Miller, J.F., and Ragsdale, C.W. (1988). *High efficiency transformation of E.coli by high voltage electroporation. Nucl. Acids. Res.* **16:**6127-6145.

Dubnau, D. (1999). *DNA uptake in bacteria. Annu. Rev. Microbiol.* **53**:217–244.

Hahn, H. P. (1997). *The type-4 pilus is the major virulence-associated adhesion of Pseudomonas aeruginosa—a review. Gene* **192**:99–108.

Fowlis, W.W. (1988) *Experimental and theoretical analysis of the rate of solvent equilibration in the hanging drop method of protein crystal growth. J. Crystal Growth.* **90:**117-129.

Fulcher, N., Holliday, P., Klem, E., Cann, M., and Wolfgang, M. (2010). *The Pseudomonas aeruginosa Chp chemosensory system regulates intracellular cAMP levels by modulating adenylate cyclase activity. Mol. Micro.* **76:**889-904.

Gallant, C.V., Daniels, C., Leung, J.M., Ghosh, A.S., Young, K.D., Kotra, L.P., and Burrows, L.L. (2005). *Common β-lactamases inhibit bacterial biofilm formation. Mol. Microbiol.* **58:**1012-1024.

Giltner, C.L., Habash, M., and Burrows, L.L. (2010). *Pseudomonas aeruginosa minor pilins are incorporated into type IV pili. J.Mol. Biol.* 398(3):444-61.

Hardalo, C. & Edberg, S. C. (1997). *Pseudomonas aeruginosa: assessment of risk from drinking water. Crit. Rev. Microbiol.* **23**: 47–75.

Hahn, H. P. (1997). *The type-4 pilus is the major virulence-associated adhesion of Pseudomonas aeruginosa—a review. Gene* **192**, 99–108.

Han, X., Kennan, R.M., Davies, J.K., Reddacliff, L.A., Dhungyel, O.P., Whittington, R.J., Turnbull, L., Whitchurch, C.B., and Rood, J.I. (2008). *Twitching motility is essential for virulence in Dichelobacter nodosus. J. Bacteriol.* **190:**3323-3335.

Howard, S.P., Gebhart, C., Langen, G.R., Li, G., Strozen, T.G. (2006). *Interactions between peptidoglycan and the ExeAB complex during*

assembly of the type II secretin of Aeromonas hydrophila. Mol. Microbiol. **59**:1062 – 1072.

Inclan, Y.F., Huseby, M.J., Engel, J.N. (2011). *FimL Regulates cAMP Synthesis in Pseudomonas aeruginosa. PLoS ONE* **6: e15867. doi:10.1371/ journal.pone.0015867**

Jacobs, M.A., Alwood, A., Thaipisuttikul, I., Spencer, D., Haugen, E., Ernst, S., Will, O., Kaul, R., Raymond, C., Levy, R., Chun-Rong, L., Guenthner, D., Bovee, D., Olson, M.V., and Manoil, C. (2003). *Comprehensive transposon mutant library of Pseudomonas aeruginosa. PNAS* **100:**14339-14344.

Kanack, K., Runyen-Janecky, L., Ferrell, E., Suh, S., and West, S. (2006). *Characterization of DNA-binding specificity and analysis of binding sites of the Pseudomonas aeruginosa global regulator, Vfr, a homolog of the Escherichia coli cAMP receptor protein. Microbiol.* **152:**3485-3469.

Koag, M., Fenton, R.D., Wilkens, S., and T.J. Close. (2003). *The binding of Maize DHN1 to Lipid Vesicles. Gain of Structure and Lipid Specificity. Plant Physiol.***131**:309-316.

Koo, J., Tammam, S., Ku, S., Sampaleanu, L., Burrows, L.L., and Howell, P.L. (2008). *PilF is an outer membrane lipoprotein required for multimerization and localization of the Pseudomonas aeruginosa type IV pilus secretin. J. Bacteriol.* **190**:6961 – 6969.

Koster, M., Bitter, W., de Cock, H., Allaoui, A., Cornelis, G.R., & Tommassen, J (1997). *The outer membrane component, YscC, of the Yop secretion machinery of Yersinia enterocolitica forms a ring-shaped multimeric complex. Mol. Microbiol.* **26**, 789–797.

Lara, B., Rico, A. I., Petruzzelli, S., Santona, A., Dumas, J., Biton, J. et al. (2005). *Cell division in cocci: localization and properties of the Streptococcus pneu- moniae FtsA protein. Mol. Microbiol.* **55**:699–711.

Lewenza, S., Falsafi, R.K., Winsor, G., Gooderham, W.J., McPhee, J.B., Brinkman, F.S., and Hancock, R.E. (2005). *Construction of a mini-Tn5- luxCDABE mutant library in Pseudomonas aeruginosa PAO1: a tool for identifying differentially regulated genes. Genome Res.* **15:**583-589.

Lautrop, H (1961). *Bacterium anitratum transferred to the genus Cytophaga. Int. Bull. Bacteriol. Nomencl.* **11**:107–8.

Linderoth, N.A., Simon, M.N., & Russel, M (1997). *The filamentous phage pIV multimer visualized by scanning transmission elec- tron microscopy. Science* **278**, 1635–1638.

Magliery, T.J. and Regan, L. (2004). *Beyond Consensus: Statistical Free Energies Reveal Hidden Interactions in the Design of a TPR Motif. J. Mol. Biol.* **343**:731 – 745.

Maier, B., Potter, L., So, M., Seifert, H.S. and Sheetz, M.P. (2002). *Single pilus motor forces exceed 100 pN. PNAS* **99:**16012-16017.

Main, E.R.G., Xiong, Y., Cocco, M.J., D'Andrea, L., and Regan, L. (2003). *Design of Stable Helical Arrays from an Idealized TPR Motif. Struct.* **11**:497-508.

Martin, P. R., Watson, A. A., McCaul, T. F. & Mattick, J. S. (1995). *Characterization of a five-gene cluster required for the biogenesis of type 4 fimbriae in Pseudomonas aeruginosa. Mol. Microbiol.* **16:**497–508.

Mattick, J.S. (2002). *Type IV Pili and Twitching Motility. Annu. Rev. Microbiol.* **56:**289–314.

Merz, A.J., So, M., and Sheetz, M.P. (2000). *Pilus retraction powers bacterial twitching motility. Nature* **407**:98-102.

Michel, G.P.F., Aguzzi, A., Ball, G., Soscia, C., Bleves, S., and Voulhoux, R. (2011) *Role of fimV in type II secretion system-dependent protein secretion of Pseudomonas aeruginosa on solid medium. Microbiology.* **157**:1945-1954.

Mittl, P.R.E. and Schneider-Brachert, W. (2006). *Sel1-like repeat proteins in signal transduction. Rev. Cell. Signal.* **19**:20-31.

Montelione, G.T., Zheng, D., Huang, Y.J., Gunsalus, K.C., Szyperski, T. (2000). *Protein NMR spectroscopy in structural genomics. Nat. Struct. Biol.* **Nov**:982-985.

Morand, P.C., Bille, E., Morelle, S., Eugene, E., Beretti, J.L., Wolgang, M., Meyer, T.F., Koomey, M., and Nassif, X. (2004). *Type IV pilus retraction in pathogenic Neisseria is regulated by the PilC proteins. EMBO J.* **23:**2009-2017.

Nguyen, Y., Jackson, S.G., Aidoo, F., Junop, M., and Burrows, L.L. (2009). *Structural Characterization of Novel Pseudomonas aeruginosa Type IV Pilins. J. Mol. Biol.* **395**:491-503.

Nickel, J.C., Ruseska, I., Wright, J.B., Costerton, J.W. (1985). *Tobramycin Resistance of Pseudomonas aeruginosa Cells Growing as a Biofilm on Urinary Catheter Material. Antimicrob. Agents Chemother.* **27**: 619-624

Nunn, D., Bergman, S. and Lory, S. (1990). *Products of three accessory genes, pilB, pilC, and pilD, are required for biogenesis of Pseudomonas aeruginosa pili. J. Bacteriol.* **172:**2911 – 2919.

Oldfield, N.J., Bland, S.J., Taraktsoglou, M., Ramos, F.J., Robinson, K., Wooldridge, K.G., Ala'Aldeen, D.A.A. (2007) *T-cell stimulating protein A (TspA) of Neisseria meningitidis is required for optimal adhesion to human cells. Cell. Microbiol.* **9:**463 – 478.

O'Toole, G. A. and Kolter, R. (1998). *Flagellar and twitching motility are necessary for Pseudomonas aeruginosa biofilm development. Mol. Microbiol.* **30**:295–304.

Parge, H. E., D. E. McRee, M. A. Capozza, S. L. Bernstein, E. D. Getzoff, and J. A. Tainer. (1987). *Three dimensional structure of bacterial pili. Antonie Leeuwenhoek* **53**:447–453.

Peabody, C.R., Chung, Y.J., Yen, M., Vidal-Ingigliardi, D., Pugsley, A.P., and Saier, M.H. Jr. (2003). *Type II protein secretion and its relationship to bacterial type IV pili and archaeal flagella. Rev. Microbiol.* **149**:3051–3072.

Provencher, S.W. and Glockner, J. (1981). *Estimation of Globular Protein Secondary Structure from Circular Dichroism. Biochem.* **3**:297-317.

Rual, J., et al. (2005) *Towards a proteome-scale map of the human protein–protein interaction network. Letters to Nat.* **437: doi:10.1038/nature04209**

Russell, M.A., and Darzins, A. (1994). *The pilE gene product of Pseudomonas aeruginosa, required for pilus biogenesis, shares amino acid sequence identity with the N-termini of type 4 prepillin proteins. Mol. Microbiol.* **13:**973-985.

Sampaleanu, L.M., Bonanno, J.B., Ayers, M., Koo, J., Tammam, S., Burley, S.K., Almo, S.C., Burrows, L.L., and Howell, P.L. (2009). *Periplasmic Domains of Pseudomonas aeruginosa PilN and PilO Form a Stable Heterodimeric Complex. J. Mol. Biol.* **394**:143 – 159.

Sato , H., Okinaga, K., and Saito H. (1988). *Role of pili in the pathogenesis of Pseudomonas aeruginosa burn infection.* Microbiol. Immunol. **32**:131-139.

Seifert, H. S., Ajioka, R. S., Marchal, C., Sparling, P. F. and So, M. (1988) *DNA transformation leads to pilin antigenic variation in Neisseria gonorrhoeae. Nature* **336**:392–395.

Scheurwater, E. M., and A. J. Clarke (2008). *The C-terminal domain of Escherichia coli YfhD functions as a lytic transglycosylase. J. Biol. Chem.* **283:**8363–8373.

Semmler, A.B., Whitchurch C.B., and Mattick, J.S. (1999). *A re-examination of twitching motility in Pseudomonas aeruginosa. Microbiol.* **145:**2863-2873.

Semmler, A.B.T., Whitchurch, C.B., Leech, A.J., and Mattick, J.S. (2000). *Identification of a novel gene, fimV, involved in twitching motility in Pseudomonas aeruginosa.* Microbiol. **146**:1321-1332.

Slingsby, C., Bateman, O.A., and Simpson, A. (1993). *Motifs involved in protein-protein interactions. Mol. Biol. Rep.* **17**:185 – 196.

Strom, M.S., Lory S. (1993). *Structure–function and biogenesis of the type IV pili. Annu Rev Microbiol* **47***:* 565–596.

Touhami, A., Jericho, M.H., Boyd, J.M., and Beveridge T.J. (2006). *Nanoscale characterization and determination of adhesion forces of Pseudomonas aeruginosa pili by using atomic force microscopy. J. Bacteriol.* **188:**370-377.

Tammam, S., Burrows, L., and Howell, L. (2011) Manuscript Submitted

Varga, J.J., Nguyen, V., O'Brien, D.K., Rodgers, K., Walker, R.A., and Melville, S.B. (2006). *Type IV pili-dependent gliding motility in the Gram-positive pathogen Clostridium perfringens and other Clostridia. Mol.Mircobio.* **62**:680–694.

Wehbi, H., Portilo, E., Harvey, H., Shimkoff, A., Scheurwater, E., Howell, L., and Burrows, L. (2011) *The Peptidoglycan-Binding Protein FimV Promotes Assembly of the Pseudomonas aeruginosa Type IV Pilus Secretin. J. Bacteriol.* **193**:540-550.

Whitchurch, C.B. et al. (2004) *Characterization of a complex chemosensory signal transduction system which controls twitching motility in Pseudomonas aeruginosa. Mol. Microbiol.* **52:** 873-893.

Zolfaghar, I., Evans, D.J., and Fleiszig, S.M.J. (2003). *Twitching motility contributes to the role of pili in corneal infection by Pseudomonas aeruginosa. Infect. Immun.* **71:**5389-5393.